IN-SITU X-RAY STUDIES OF THE UNDERPOTENTIAL DEPOSITION OF COPPER ON PLATINUM (111)

by

Howell S. Yee and Héctor D. Abruña *

Department of Chemistry
Baker Laboratory
Cornell University
Ithaca, NY 14853-1301

ABSTRACT In-situ x-ray flourescence detected surface EXAFS spectroscopy has been employed to elucidate the in-plane structure of copper underpotentially deposited on a clean and well ordered platinum (111) single crystal electrode. XANES and EXAFS analyses were made as function of applied potential (+0.2V, +0.1V, and 0.0V) corresponding to coverages of approximately 0.5ML, 0.75ML and 1ML, respectively. The charge derived from electrochemical measurements indicate that at the three potentials studied the electrodeposited copper was not completely discharged. The XANES analysis revealed similarities between the electrodeposited copper and the Cu_2O reference lending support to earlier findings of a partially discharged copper ad-layer. EXAFS results suggest two cluster phases at the most positive potential (+0.2V) studied and an epitaxial arrangement at the most negative potential (0.0V).

INTRODUCTION

Investigations of metal adsorbates in the submonolayer and monolayer regimes on metallic and semiconducting substrates have played a dominant role in surface science for the past two decades. The presence of metal adsorbates can profoundly affect the structural, optical and electronic properties of the substrate. For instance the adsorbate can cause surface reconstructions, work function changes, charge transfer, change in the dielectric constants and others. [1]

Two methods are primarily employed for depositing submonolayer and monolayer amounts of a metal onto a substrate and these involve ultra-high vacuum (UHV) and electrochemical means. In the ultra-high vacuum environment deposition occurs via vaporization of a metal source, whereas the electrochemical method is based on so-called underpotential deposition (UPD). In underpotential deposition, a metal can be electrodeposited on a foreign metal substrate at potentials significantly more positive than that for deposition on the same metal surface. The process of underpotential deposition provides one of the most precise means of controlling coverages from submonolayer to monolayer and in some cases multilayer coverages in a quantifiable and reproducible fashion prior to bulk deposition. Over the past two decades extensive studies have been undertaken to understand this phenomenon due to its theoretical and technological ramifications such as observations of molecular vs. bulk properties, electrocrystallization, catalysis and surface chemistry and physics.

Numerous electrochemical and spectroscopic techniques have been brought to bear on the questions of the mechanism(s) of monolayer formation as well as structural properties of the UPD layer. Cyclic voltammetry and potentiostatic current transients[2] have been employed to obtain thermodynamic and kinetic information about the UPD process. Structural characteristics

of the UPD layer have been indirectly derived from equilibrium-coverage potential isotherms.[3] Although electrochemical techniques have provided a wealth of information, structural inferences have been indirect and model dependent.

Atomic structural details have been reported using surface sensitive ultra high vacuum methods and much data have been obtained from them.[4] Various electron spectroscopic techniques have been employed in the structural study of copper UPD on an iodine pretreated Pt(111) surface.[4b] Due to the inherent nature of the experiments, the electrode had to be emersed from solution. Upon emersion, potential control is lost thus introducing questions regarding the integrity of the double layer. In addition, it is uncertain what structural changes the UPD adlayer might undergo during the course of transfer from solution to vacuum. Although these ex-situ experiments have provided an abundance of information, certain questions remain unanswered and their relation to electrochemical interfaces is still a matter of debate.

The advent of atomic resolution microscopies, scanning tunneling (STM) and atomic force (AFM), have allowed for direct atomic structural measurements, in-situ, on UPD systems. STM and AFM have been employed to study UPD processes of copper on gold and platinum electrodes[5a-e] and silver and bismuth on gold surfaces.[5f] These studies showed that the UPD process occurred in a well defined manner and that the adlayer structures observed were similar to those observed in vacuum. Despite the success and power of STM and AFM, information regarding the solution side of the interface is still lacking. Weakly adsorbed electrolyte species have not been observed (and it is unlikely that they will be with STM or AFM) despite radiotracer studies by Wieckowski and co-workers[6] that have shown an enhanced adsorption of HSO_4^- during copper UPD on platinum. The lack of any evidence of weakly adsorbed HSO_4^-

from STM or AFM studies might suggest that the probe's tip perturbs these weakly adsorbed species in some manner or that they are too mobile to be imaged.

Recently, with greater access to synchrotron facilities, in-situ x-ray spectroscopic and diffraction techniques have opened a unique window to atomic structural information of UPD systems in a non-invasive manner.[9,10,11,12] Extended x-ray absorption fine structure (EXAFS), surface EXAFS and x-ray absorption near edge structure (XANES) have been used to study various UPD systems.[10] Information on local structure, atomic environment and oxidation state of the adsorbed species has been obtained. Such studies have led to the observation of adsorbed oxygen containing species (either from the solvent or the electrolyte) on the UPD adlayer,[10] not observed with either STM or AFM, and consistent with partial charge transfer. Specific systems that have been studied include Cu on Au(111) and Au(100), Cu on Pt(100), Pt(111)-I and polycrystalline platinum, Ag on Au(111), Pb on Ag(111) and others.[10] In-plane structural measurements of the UPD layer were made using grazing incident x-ray scattering for specific systems.[11] In addition, the use of x-rays in the production of a standing wave field normal to the surface, has allowed the electrical double layer to be directly probed.[12]

In the present paper, we describe our results from an in-plane structural study of the underpotential deposition of copper onto a clean and well-ordered Pt(111) surface. Potential dependent structural changes were determined in-situ by means of XAS in the flourescence detection mode. The results suggest two cluster phases at the most positive potential (+0.2V) studied and an epitaxial arrangement at the most negative potential (0.0V).

EXPERIMENTAL

Measurements were conducted at the B-2 station of the Cornell High Energy Synchrotron Source (CHESS) using a Si(111) double crystal monochromator. The incident beam was collimated with a pair of motorized hutch slits and Huber slits just before the sample. The incident beam intensity was monitored with an ionization chamber with nitrogen as the fill gas. The Cu (K_α) fluorescence was monitored using an energy dispersive Si(Li) detector (Princeton Gamma Tech) in conjunction with a EG&G 673 Spectroscopy Amplifier. A single channel analyzer (Tennelec) served to discriminate against the background and other undesirable contributions to the signal. A thin lead slit placed directly in front of the detector served to reduce the total counts at the detector and enhanced the signal to noise ratio.

Spectra were collected using the CHESS data acquisition program SPEC. All measurements were taken in-plane (σ-polarization) at grazing incidence. The angle that the incident beam made relative to the sample was approximately 5 mrad. X-ray absorption spectra were recorded at the Cu K edge, at 8980 eV. The EXAFS spectra were collected in a 1000 eV window from 8800 eV to 9800 eV. Within the 1000 eV window three regions were defined, 8800 - 8900 eV, 8900 - 9100 eV, and 9100 - 9800 eV. The step/energy interval for the region 8900 - 9100 eV was 2 eV and 4 eV for the others.

Data were collected in scans of 20 - 30 minutes. Typically 20 scans were collected and averaged to obtain a reasonable signal to noise ratio. The major inflection point in the edge jump was taken to be the position of the edge. Standard analysis of the data consisted of background subtraction, normalization, truncation of the data set at approximately 20 eV above the edge, conversion of the energy E-scale to wavenumber k-scale, and a k weighing ($k^l \cdot \chi(k)$) of the data from k = 3 to 13 Å^{-1}. Fourier filtering of only the first shell contribution to the EXAFS

signal was performed. Bond distances were obtained by fitting the oscillatory part of the EXAFS equation to the experimental oscillations with the phase shift for the pair of interest being obtained experimentally from reference compounds. The spectra of Cu foil, Cu_2O, $CuSO_4$, and CuO, used as reference compounds, were measured in transmission mode. The spectrum of a bulk Pt_3Cu alloy was measured in fluorescence mode. Further analysis of the data was carried out with BAN and MFIT (Tolmar Instruments) a commercial EXAFS analysis package.

The electrochemical cell, contained inside an aluminum housing, consisted of a cylindrical Teflon body with feedthroughs for electrolytes and electrode connections. A thin-layer of solution (of approximately 5 μm) was trapped between the electrode and a 6 μm thick polypropylene film, held in place by a viton O-ring. The film was distended by introducing electrolyte to allow deposition from the bulk solution. Afterwards, the thin-layer configuration was re-established by the removal of electrolyte. Solutions were introduced into the cell with solution bubblers. The aluminum housing was continuously flushed with prepurified nitrogen gas, thus ensuring that the effects of oxygen diffusion through the polypropylene would be minimal. The entire cell, with aluminum housing, was mounted on a Huber goniometer stage which allowed for very precise angular motion as well as vertical and horizontal translation of the sample.

The cylindrical Teflon body was designed to ensure complete rinsing of the cell and crystal as would be necessary when co-adsorbing anions were deliberately introduced into the cell. However, as a result of such a design, both faces and the edges of the Pt(111) crystal were exposed to the electrolyte. Although electrochemical process occurred on the two faces and the edges, the x-ray interacted only with the top face.

The electrochemical equipment consisted of a BAS CV-27 potentiostat and voltammograms were recorded on a Soltec X-Y recorder. All potentials were measured against a Ag/AgCl reference electrode without regards to the liquid junction.

Solutions were prepared using high purity 18 MOhm Millipore Milli-Q water. Aqueous acid solutions were prepared from high-purity (Ultrex) sulfuric acid. Copper ion solutions were prepared by dissolution of $CuSO_4 \cdot 5H_2O$ (Aldrich Gold Label) in sulfuric acid. Prior to introduction into the electrochemical cell, the solutions were degassed with pre-purified nitrogen gas which was passed through hydrocarbon and oxygen traps (MG Industries). The chemical composition of the electrolytic solution was $0.1\underline{M}$ H_2SO_4, $50 \times 10^{-6}\underline{M}$ Cu^{2+}. The low Cu^{2+} ion concentration was necessary to ensure negligible contribution to the background fluorescence signal. In the thin-layer configuration at all potentials studied, we calculated that less than 5 % of the absorbing copper atoms are present as ions in the electrolyte. XAS scans were also collected at the rest potential of the system.

The Pt(111) crystal disk (10 mm diameter and 1.5 mm thickness) used in the XAS experiments was grown from the melt at the Cornell University Materials Preparation Facility. The crystal was oriented by Laue photography, and then chemically and metallographically polished. Electrode surface pretreatment involved immersion in hot concentrated nitric acid for 5 hours, followed by rinsing with Milli-Q high purity water. Annealing of the Pt crystal involved placing the Pt disk in a Pt ladle specifically designed for the Pt disk (Micky Roof Designer Goldsmith). The Pt crystal was annealed under a CH_4 - O_2 flame for 6 minutes followed by cooling under a stream of prepurified nitrogen gas for 2 minutes before immersion into a degassed solution of $0.1\underline{M}$ H_2SO_4. This procedure avoided the problem of strains induced by the rapid quenching and produced a clean and well ordered Pt(111) surface as evident by the

voltammogram in 0.1M H_2SO_4 shown in figure 1. The Pt(111) crystal was then transferred to the electrochemical cell under the protective cover of a "ladle full" of electrolyte (0.1M H_2SO_4). Electrical contact to the disk was made with an embedded Pt wire. The Pt(111) crystal was secured by 3 pressure points in the Teflon body.

The experimental setup ensured the integrity of the clean and well-ordered Pt(111) surface for extended time periods. Thus, the crystal needed to be annealed approximately once during any 24 hour period. Cyclic voltammetric scans of the Pt(111) crystal in 0.1M H_2SO_4 were taken every 2 hours to verify the presence of a clean and well-ordered Pt(111) surface.

Underpotential deposition of copper from the dilute (50×10^{-6}M) aqueous solution of Cu^{2+} in 0.1M H_2SO_4 was carried out by sweeping the applied potential negatively from the rest potential, typically about +0.7V, at a rate of 2 mV/s. For XAS measurements the potential was then held at +0.2V, +0.1V and 0.0V where XAS measurements were made. The copper upd layer was stripped and re-deposited after collecting two XAS scans (1 hour period). Before deposition of copper, the cell was rinsed thoroughly with 0.1M H_2SO_4. This procedure ensured that time dependent changes of the adlayer would not be measured and, if present, would be detected electrochemically.

The charge corresponding to the stripping of the electrodeposited copper was used in calculating the coverage values which are presented in Table 1. In these calculations it was assumed that the copper had an electrosorption valency of two; that is complete discharge of copper. In addition, no correction was made for the difference in the potential of zero charge as this would be a small effect on the calculated charge.

RESULTS

Electrochemistry

UPD refers to the electrodeposition of metal monolayer(s) on a foreign metal substrate at potentials significantly more positive than that for deposition on the same metal surface. This allows for a precise control of the surface coverage prior to the onset of bulk deposition at which point the deposition is driven by the Nernst equilibrium. Structural studies within the UPD regime can provide a wealth of information on nucleation processes, coverage dependent structure and electronic properties of a metallic adlayer.

In order to establish the cleanliness and order of the Pt(111) electrode, a cyclic voltammogram was run in 0.1M H_2SO_4. The voltammetry in figure 1 displays features that are associated with a clean, well-ordered Pt(111) surface otherwise known as the "butterfly" pattern.[16, 17, 18] The scan was initiated from the rest potential (+0.70V) at 50 mV/s proceeding into the cathodic region and reversed at -0.18V. Subsequent scans were cycled within the limits of +0.65 and -0.18V, respectively. The voltammetric features at potentials below 0 volts are attributed to the edges of the crystal which were also exposed to the solution. Despite repeated stripping, underpotential deposition of copper, and rinsing with 0.1M H_2SO_4 the surface of the Pt(111) crystal remained clean and well ordered for extended time periods as ascertained from voltammetric measurements.

Figures 2a-d show the underpotential deposition of copper under the various experimental conditions of interest. All scans were initiated at the rest potential and proceeded in the negative direction to the potential of interest. Voltammetric scans were conducted both in a standard electrochemical cell with dipping configuration (Fig 2a) as well as in the XAS cell (Fig. 2b-d) in order to compare the two. There are essentially no differences between the two voltammetries

other than the increased charged measured in the XAS configuration due to exposure of the entire crystal to the copper solution. In both experimental configurations the deposition is diffusion limited due to the low concentration of Cu^{2+} ions (50 x 10^{-6}M). In addition, because of the low copper ion concentration, 50 x 10^{-6}M, no deposition peaks were observed, as anticipated. However, under both experimental conditions the stripping peaks were well defined.

From Table 1 it can be seen, and as anticipated, that the measured charge of the anodic (stripping) peak increased upon holding the potential at 0.0 V from +0.2V. It is interesting to note that neither the charge at 0.0V nor at +0.1V corresponded to a complete monolayer of fully discharged Cu^{2+} which would be 420 $\mu C/cm^2$. It has been suggested that the electrosorption valency for copper deposition on Pt is less than two, that is, there is partial charge transfer. In addition, recent studies[4d, 10h, 10i, 24] have shown that some of the adsorbed copper may exist in a non-electroactive form, and thus would not contribute to the anodic peak.

Voltammetry for the UPD of copper at 50 x 10^{-6}M in the presence of chloride at 10^{-3}M is shown in figure 3. As noted by several groups[24] chloride does not adsorb as strongly as iodide to platinum as evidenced by the ability to rinse the chloride from the platinum surface. Unlike the co-adsorption studies with iodide[4b, 10d, 12d] where the platinum surface was pretreated with iodide prior to exposure to the copper electrolyte solution, the underpotential deposition of copper was conducted in the presence of chloride ions in solution. Thus this can be viewed as a true competitive adsorption process. Unlike the voltammetry in the absence of chloride where the cathodic features were not very evident, the voltammetry in the presence of chloride gave rise to two somewhat broadened peaks. It is clear that the presence of chloride greatly influences the deposition process as demonstrated in the voltammetric responses. The anodic features of the

Cu/Cl voltammetry are similar to those reported by White and Abruña[24a] and Kolb *et al.*[24b] The charge under the two peaks corresponds to that under the singular peak for Cu stripping (Fig 2c. Table 1) in the absence of chloride. It should be noted that the design of the XAS cell allowed for complete rinsing of all chloride from the system restoring the voltammetry of a clean and well-ordered Pt(111) electrode in 0.1M H_2SO_4. Further discussion on the Pt(111)-copper-chloride system will be presented elsewhere.[26]

XANES Information

Useful qualitative information can be extracted from examination of the threshold position and near edge features of the spectrum as they are very sensitive to the electronic state and environment of the absorbing atom. Near edge information can also provide a means of selecting reference compounds for use in the complete EXAFS analysis. The near edge features of three of the reference compounds employed, copper foil, Cu_2O and the Pt_3Cu alloy bear a strong similarity to those for the *in-situ* Pt(111)/Cu XAS data. Figures 4a - 4c present data for the reference compounds and the UPD copper at the various potentials as indicated. For all data sets the threshold position (0 eV) was consistently taken to be the inflection point (pre-peak) along the Cu *K* edge.

The edge profile of copper foil (Figure 4a) shows a pre-peak feature and two additional peaks at approximately 10 eV and 20 eV beyond threshold. For Cu_2O (i.e. Cu^+) (Figure 4a) the edge profile displays a pre-peak which is slightly enhanced, as well as additional peaks at about 10 eV and 27 eV with the latter being somewhat broad. In the Pt_3Cu alloy the pre-peak feature is greatly diminished in comparison to metallic copper and Cu_2O. The alloy also has strong edge features at 7 eV and 30 eV with a noticeable shoulder at 12 eV.

At all three potentials studied (Figures 4a-c) there is a strong similarity in near edge features between the in-situ measurements and the Pt_3Cu alloy. From this observation one can qualitatively state that the underpotentially deposited copper is in an environment quite similar to that of copper in the Pt_3Cu alloy. Based on these similarities and on the polarization of the x-ray beam relative to the surface it is reasonable to surmise that the copper adatoms might be located in either a three-fold hollow site or in a bridge site (but not atop sites) because of the strong Cu - Pt interaction. However, a definitive assignment of the copper position will not be possible without XAS data in the π-polarization, that is with the electric field vector normal to the surface.

The XANES features of the *in-situ* spectra for Pt(111) / Cu (at all potentials) are broad relative to those in the Pt_3Cu alloy. The intensities of the peaks at approximately 7 eV and 33 eV decrease as the applied potential changes from 0.0V to +0.2V. A shoulder at 15 eV grows as the potential decreases from +0.2V to 0.0V. The energy separation of the two peaks in the in-situ measurements is approximately the same as in the Cu_2O (Cu^+) reference compound. However, the pre-peak features, present at all three potentials, do not resemble those in the Pt_3Cu alloy but bear a strong resemblance to those in metallic copper and Cu_2O. It is quite probable that the oxidation state of the copper adlayer is somewhere between 0 and +1. As noted earlier, the measured charges are all lower than would be expected for a fully discharged monolayer consistent with a residual charge on the copper ad-layer. Thus, the XANES observations and electrochemical charge data are consistent with a copper ad-layer that is not fully discharged; that is, there is partial charge transfer.

EXAFS Information

EXAFS spectra were collected at four different potentials: +0.65V (rest potential), +0.2V, +0.1V and 0.0V. Table 1 shows the measured charges at each potential. At the rest potential no copper should be electrodeposited. Thus, the copper fluorescence signal should be negligible and due only to the copper (50μM) ions in solution. Such a background scan is shown in figure 5. A barely discernible (above background) peak is observed and, as alluded to above, is more than likely due to the copper ions in solution. This also underscores the point that its contribution to the overall signal is negligible.

The raw EXAFS spectra at 0.0V, +0.1V and +0.2V are shown in figures 6a-c, respectively. The differences in the spectral features can be attributed to variations in the local environment around the absorbing copper atoms. In addition to the very low count rate observed as background (vide-supra), the absence of a characteristic absorption (white line) just above the edge provides further evidence that the EXAFS signal arises from the adsorbed monolayer and not from Cu^{2+} in the thin layer of electrolyte. In figures 6a-c, there is an enhancement in the amplitude of the EXAFS oscillations with decreasing potential. This is consistent with the higher coverage at the more negative potentials. As the coverage increases we observe a spectrum indicative of a higher coordination number environment as compared to the low coverage spectrum. At +0.2V, which corresponds to approximately a half monolayer coverage of copper, EXAFS oscillations are still present. This indicates that even at relatively low coverage, there is still some degree of ordering in the copper adlayer. Similar results of EXAFS oscillations at submonolayer coverage have been previously reported by Abruña and co-workers[10d,e] and Tourillon and co-workers.[10j,k] As noted earlier, a pre-edge peak is present in the EXAFS spectra

at all potentials which would suggest metallic copper, but does not discount the presence of partially charged copper.

Figures 7a and 7b compare the EXAFS spectra for the underpotential deposition of copper in the absence and in the presence of chloride, respectively. In the presence of chloride, the near edge pre-peak feature is no longer present or, it is at best, barely discernible. However, the absence of a pre-peak in the presence of chloride does not necessarily imply that the deposited copper has no metallic character. Another noticeable difference is the appearance of a double peak at approximately 8990 eV for UPD of copper in the presence of chloride. In the absence of chloride, a slight shoulder is visible, which becomes more defined in the presence of chloride. Further discussion on the Pt(111) - Cu - Cl system will be presented elsewhere.[26]

More detailed structural information about the Pt(111) - Cu system can be obtained by examining the background subtracted data and the Fourier transformed and filtered data of the EXAFS spectra at the various potentials studied. Figures 8 to 10 show the Fourier analysis of the spectra obtained at 0.0V, +0.1V and +0.2V, respectively. More specifically, figures 8 - 10 (a,b) show in the top panel, the radial distribution function RDF whereas in the bottom panel, the background subtracted data (filled circles), the back Fourier transform of the windowed peak in the RDF (open circles) and the amplitude envelope (open inverted triangles) are presented. All of the data sets as well as data for the reference compounds were k=1 weighted. In all of the radial distribution functions (not phase corrected) the predominant peaks appear between 1.5 Å - 3 Å.

Radial Distribution and k^l Weighted Data

Several observations can be made regarding the radial distributions and the k weighted ($k^l \cdot \chi(k)$) data (over the range of k = 3 to 13Å^{-1}). The radial distributions show numerous unresolved peaks throughout the entire region. In the region of 2-3 Å where one would expect to find the first copper-copper nearest neighbor distances, the peak form is complex, the shells are not isolated and they often interfere with one another. Within this particular region there can be several different atomic species comprising this particular coordination shell.

When the potential is increased from 0.0V to +0.2V, the peaks in the radial distribution function between 2 Å and 3 Å show markedly different forms. The radial distribution at 0.0V shows an additional peak at approximately 1.5 Å which is not present, or not as evident, at the other two potentials. At the most positive potential (+0.2V) several shoulders are present around 1.5 Å giving rise to a rather complex spectrum. Beyond 3Å the spectra become increasingly more complicated. Additional asymmetric peaks are present as a result of interference from other atoms, shell contributions and others. No attempt was made to extract structural information beyond 3 Å. It should be stated that these are not phase corrected values, so this represents real distances of up to at least 3.5 to 4 Å.

Recent findings by Abruña *et al.*[12d] can help in understanding some of the complex features in the radial distributions. Using x-ray standing waves to study copper UPD on an iodine treated platinum surface (from a Pt/C multilayer), they observed an accumulation of copper near the surface of the platinum electrode. The amount of accumulated copper (up to about a monolayer) is potential dependent and in all cases is present in close proximity to the surface (less than 40 Å). This layer of copper is likely present in a disordered manner and, in addition, its interaction with the surface is relatively weak so that it does not survive rinsing with

supporting electrolyte. If we assume that a comparable amount of accumulated copper is also present in our system, then it may give rise to a "smearing" effect in the radial distribution because of its disordered nature. This could, in turn, cause a shift in the positions of the peaks in the radial distribution. In addition, this disordered layer could also give rise to unrealistic Debye-Waller factors.

From the geometry of the experiment (σ-polarization with copper as the absorber atom) and the limited number of species (copper, platinum and oxygen) that can serve as backscatterers, it is possible to identify the chemical species that are contributing to the complex features in the radial distribution. For example, for oxygen to be considered as one of the backscatterers would imply that they occupy either bridge or three-fold hollow sites with respect to the copper adlayer. Another, although less likely possibility would place the oxygen directly in contact with the platinum substrate. The source of oxygen could arise from either the solvent (H_2O) or from the supporting electrolyte (HSO_4^-). Copper backscatterers would place the coppers either in a 3-D cluster arrangement or as an adlattice covering the surface. Platinum backscattering would mean that the copper absorber resides in either bridge or three-fold-hollow sites but not an atop site with respect to the substrate. Keeping these points in mind, we discuss our findings of the structure of the copper UPD layer at the various potentials (and thus coverages) studied.

Pt(111) with Cu deposited at 0.0V:

We begin with results obtained at 0.0V which represents approximately a monolayer coverage of copper on the platinum surface. Figure 8a presents the magnitude of the Fourier transform obtained from the k weighted ($k^1 \cdot \chi(k)$) data in the range from k = 3 to 13 $Å^{-1}$. In

figure 8b, the open circles superimposed on the raw EXAFS (full circles) are the inverse transform of the two peaks in the RDF obtained by using a filtering function (shown in figure 8a) to isolate the range between 1.5 Å and 2.8 Å. Both the frequency and amplitude of the filtered transform fit the raw EXAFS well over the entire spectrum.

As mentioned earlier, there are potentially three species, mainly copper, oxygen and platinum which can serve as backscatterers. Although EXAFS is not very sensitive to the atomic number of the backscattering atoms, it is possible to distinguish between atoms with a large atomic number difference.

In the radial distribution function for the data at 0.0V, there are unresolved peaks, (not corrected for atom phase shifts) at 1.5 Å, 1.8 Å and 2.5 Å (Fig 8a). Assignment of the peak at 1.5 Å is somewhat uncertain at this time. It could be assigned to a copper - oxygen first nearest neighbor with a calculated distance of 1.73 Å. This value is considerably shorter than known copper-oxygen distances in various inorganic compounds.[13, 14] The distance of 1.73 Å would have to represent a projected distance. For the Cu-O distance to have a reasonable value (e.g. 2.1 - 2.2 Å) would imply that the oxygen rests at an angle of approximately 20° relative to the substrate. This suggests that the oxygen could be shared with neighboring copper atoms. Platinum was also considered as a possible backscatter that could give rise to the peak at about 1.5 Å. A distance of 1.78 Å is calculated (after phase correction) for the copper-platinum pair. Measurements in the π-polarization would allow a more precise determination of the number of nearest platinum neighbors. This, along with the backscattering envelope (which allows a distinction between a high and a low atomic number backscatterer) would allow an unambiguous assignment of this peak. However, at this time we can only speculate as to the possible assignment of this peak. In a number of studies on the Cu UPD on Au(111) system[10a,b,j,k] the

copper atoms have been found to reside on three-fold-hollow sites. This is the energetically most favorable state and thus it is very likely that the copper also resides in the three-fold-hollow sites of Pt(111).

Fourier filtering of the composite peaks at 1.8 Å and 2.5 Å (not corrected for phase shift) was considered next. Two factors could give rise to the unresolved peaks. One possibility is that several different atomic species constitute a coordination shell or, alternatively, that there are two coordination shells that are not completely resolved.

The unresolved minor peak at 1.8 Å was windowed along with the more prominent one at 2.5 Å. The amplitude envelope showed a beat node at 8 $Å^{-1}$. A beat node between 6 to 8 $Å^{-1}$ is a strong indicator of a heavy atom scatterer which in the present context could only be platinum. Though a beat node is not a requisite (it can also be due to multiple shells or several different atomic species), it does however, lend credence to the notion that platinum is a backscatter and that the copper atoms occupy either bridge or three-fold hollow sites on the platinum surface. Deposition onto top-sites can be disregarded since given the polarization employed, the platinum would not contribute any scattering. When the unresolved peaks were fitted using the copper-copper 1st shell reference and the copper-platinum reference, distances of 2.14 Å and 2.86 Å were obtained for cooper-copper and copper-platinum, respectively. A (projected) copper-copper bond distance of 2.14 Å would require that the backscattering copper be resting on the absorbing copper at an angle of approximately 30° with respect to the substrate. A copper-platinum distance of 2.86 Å appears somewhat unrealistic considering the geometry of the system and since it is significantly larger than what is normally accepted as a copper platinum bond distance. Based primarily on the copper-platinum distance the above interpretation was rejected.

As mentioned above, the presence of a beat node is also consistent with the presence of multiple shells or several different atomic species. In the present case, we have chosen to fit the data with oxygen and copper as backscatterers. Copper-oxygen and copper-copper bond distances of 2.16 Å (NN = 4.1 ± 20%) and 2.77 Å (NN = 6.3 ± 20%) were found. The copper-oxygen distance agrees with the various copper-oxygen bonds of $CuSO_4 \cdot 5H_2O$.[14] A distance of 2.16 Å would place the oxygen in a most interesting location that being one where the oxygen could be shared. This copper-oxygen bond is clearly different from that discussed previously where a distance of 1.73 Å was derived. The copper-copper bond length is very close to the platinum-platinum lattice spacing in the (111) direction, suggesting that the deposited copper forms a commensurate adlayer on the platinum (111) surface. Similar findings of a copper monolayer forming a commensurate layer on the Au(111) surface have also been reported[10a,b,j,k] The results from those studies also suggest that the copper atoms occupy three-fold-hollow sites.

Another plausible model would involve having copper as both the first and second nearest neighbor. In this case the calculated distances were found to be 2.21 Å and 2.77 Å, respectively. A copper-copper distance of 2.21Å is much shorter than the bulk copper-copper distance of 2.56 Å. In order to accommodate such a short distance, this copper would need to be in some sort of 3-D cluster. In such an arrangement, the first copper would reside at an angle of approximately 30° with respect to the substrate. 3-D cluster formation of copper underpotentially deposited on electrodispersed platinum has been proposed by Arvia and co-workers[25a] and on polycrystalline platinum electrode by Furuya and Motoo.[25b] The second copper-copper distance of 2.77 Å would correspond to an (1 x 1) epitaxial arrangement of copper on the platinum (111) surface.

Pt(111) with Cu deposited at +0.1V:

We next consider data at an applied potential of +0.10 V which corresponds to a copper coverage of approximately 0.75 of a monolayer and compare these results with those at 0.0V. Figure 9a shows the magnitude of the Fourier transform whereas figure 9b depicts the k weighted ($k^1 \cdot \chi(k)$) data over the range of k = 3 to 13 $Å^{-1}$ (full circles), the back Fourier transform (open circles) and the amplitude function envelope (open triangles). A noticeable difference exists between the radial distributions at 0.0V and at +0.1V. At +0.1V there is no peak at about 1.5 Å and the one at 2.5 Å has decreased in magnitude to about that of the peak at 1.8 Å which remained relatively unchanged in intensity. It would appear that the major changes in the spectra at 0.0V and +0.1V concern the peaks at 1.5 Å and 2.5 Å.

The unresolved doublet centered around 2 Å in figure 9a was fitted using copper and oxygen as backscatterers and the bond distances obtained from the fits were 2.16 Å (NN = 4.2 ± 20%) and 2.85 Å (NN = 6.2 ± 20 %) for Cu-O and Cu-Cu, respectively. The copper-oxygen bond distance is comparable to that at 0.0V. Based on this, we assume that the position of the oxygens, in relation to the copper ad-layer and the platinum substrate, is probably the same. The copper-copper distance of 2.85 Å is larger than that at 0.0V which was 2.77 Å. These findings agree with the expectation that at higher coverages (0.0V) the adlayer will assume a more compact structure and conversely, at lower coverages (+0.1V) it will take on a more open structure. The expansion of the copper adlattice with respect to the platinum substrate (2.85 Å vs. 2.77 Å) would be consistent with an arrangement that would minimize electrostatic repulsion between the partially charged copper ad-atoms.

As with the data at 0.0V, we found that we could employ a model with copper as both the first and second nearest neighbor. With such a model, distances of 2.22 Å and 2.84 Å,

respectively are obtained. A copper-copper distance of 2.22 Å is much shorter than the bulk copper-copper distance of 2.56 Å and would only be consistent with the formation of a 3-D cluster. As mentioned previously, there has been some evidence for the formation of such clusters in the UPD of copper on platinum electrodes.[25]

Within the uncertainty of the measurement (± 0.03 Å) the copper-copper distance (2.84 Å) obtained from the fit using copper as the first and second nearest neighbor is essentially the same as that (2.85 Å) obtained from the fit using oxygen and copper as backscatterers. We thus conclude that the peak at 2.84 Å (second peak) is due to copper near neighbors.

Pt(111) with Cu deposited at +0.2V:

We finally consider data at an applied potential of +0.20 V which corresponds to a copper coverage of 0.5 monolayer and compare these results with those at 0.0 and +0.1V. Figure 10a shows the magnitude of the Fourier transform and figure 10b depicts the k weighted ($k^1 \cdot \chi(k)$) data in the range from k = 3 to 13 $Å^{-1}$ (full circles), the back Fourier transform (open circles) and the amplitude function envelope (open triangles). Noticeable differences exist between the radial distribution at +0.2V and those at 0.0V and +0.1V. First, the major feature between 2 Å and 3 Å in figure 10a appears to be composed of the superposition of a number of peaks suggesting the presence of different chemical species.

The pronounced peak at about 2.2 Å was difficult to isolate because of the shoulders and unresolved peak that are very close to it. A window filtering function from approximately 1 Å to 3 Å was used to isolate the unresolved peaks. Three components were necessary in order to fit the data. The following absorber-backscatterer pairs provided the best fit: copper-oxygen,

copper-copper (1st neighbor) and copper-copper (2nd neighbor). Distances of 1.99 Å (NN = 4.3 ± 20%), 2.66 Å (NN = 6.2 ± 20%) and 2.87 Å (NN = 5.7 ± 20%); respectively were found.

The two copper-copper distances present an interesting case. The copper-copper distance of 2.66 Å was somewhat unexpected considering that at +0.2V we have about 0.5ML of copper on the surface. A copper-copper distance of 2.66 Å is significantly shorter than the copper-copper distance of 2.77 Å found at 0.0V, the potential with the highest coverage. The value of 2.66 Å is quite close to the bulk metallic copper-copper bond distance. The second nearest copper-copper bond distance of 2.87 Å is slightly longer than the value of 2.85 Å found at +0.1V. This latter one is comparable to that found by White and Abruña[10d] for a submonolayer coverage of copper on a iodine pretreated platinum surface. The two copper-copper distances suggest that there are two distinct copper adlattices present at a half monolayer coverage. The copper-copper distance of 2.66 Å is considerably smaller than the platinum-platinum bond distance in the (111) direction. Likewise the copper-copper bond length of 2.87 Å is larger than the substrate bond distance. Neither distance would suggest that the platinum substrate plays a dominant role in ordering the copper adlayer at +0.2V. This may be consistent with the formation of copper cluster as well as with an adlayer with an open structure.

DISCUSSION

Both the electrochemical and x-ray data suggest that the copper adatoms are not fully discharged (i.e. partial charge transfer). Similar observations have been reported for copper on gold[10f,j,k] and copper on platinum.[10h,i, 24] It also appears that the copper atoms might be in non-equivalent states. Such a situation could arise from either direct or indirect interactions of copper-oxygen, copper-copper or copper-platinum. The shape of the near edge features is likely

due to a superposition of various profiles, giving rise to a general similarity with the Cu^{+} edge. From the electrochemical data (Table 1), the potential at which one monolayer of copper should be present is inconsistent with the measured charge. Goodman and co-workers[4d] have reported a similar discrepancy for the same system in the UHV environment and also concluded that the copper ad-layer is not fully discharged.

Wieckowski and co-workers[7,8] and others[19, 20] have shown that on a bare single crystal platinum electrode the amount of HSO_4^- adsorbed decreases as the voltammetric scan proceeds further into the negative region (hydrogen adsorption/evolution). However, in recent radiotracer work, Wieckowski *et al.*[6] showed that there was an enhanced adsorption of HSO_4^- in the presence of electrodeposited copper. At the present time it is not clear whether the excess HSO_4^- resides on top of the copper adlayer or on the platinum surface. However, the fact that the copper species are not fully discharged may be, in part, responsible for this enhanced adsorption.

If oxygen atoms reside on atop sites, then with the σ-polarization of the x-ray employed in this study one would not expect oxygen to play a significant role as a backscatter. If copper-oxygen scattering is responsible for the first peak in the unresolved doublets, it would imply that the oxygen occupies a position other than atop site. Earlier studies of the underpotential deposition of copper on gold (111) found oxygen to reside on atop sites.[10a] The data strongly indicate that oxygen is a backscatter, with the source of oxygen being either the solvent (water) or the electrolyte (0.1M H_2SO_4). In the present study we see strong scattering by oxygen (which implies that the Cu-O bond has an in-plane projection) and we obtain a copper-oxygen distance of 2.16 Å. The fact that scattering by oxygen is observed implies that

there is a projection of the Cu-O bond in the plane; thus excluding atop sites. This would leave bridge and three-fold hollow sites as possible locations for the oxygen.

Recent findings of Durand *et al.*[10i] and Furtak *et al.*[10g] on the underpotential deposition of copper on Pt(100) and polycrystalline platinum, respectively, showed strong evidence of in-plane oxygen backscattering. In the work by Tadjeddine *et al.*[10j] on copper UPD on Au(111), a pronounced peak present at approximately 1.9 Å was attributed to oxygen backscattering. Thus, there is clear precedent for oxygens occupying positions other than atop sites.

However, several differences should be noted with regards to the recent study of copper UPD on the Pt(100) surface[10i] and our study. The two major differences are the crystallographic orientation of the electrode and the supporting electrolyte employed. Durand *et al.* used a mixture of $NaClO_4$ / $HClO_4$ as the supporting electrolyte. Unlike HSO_4^-, ClO_4^- is not strongly adsorbed onto platinum. Their voltammetry for copper deposition differed greatly from that presented in this study in terms of peak sharpness. It is difficult to ascertain the quality of the Pt(100) crystal employed by Durand *et al.* without a voltammogram in the absence of copper. As noted earlier, we have ensured that at all times we had a clean and well-ordered Pt(111) surface as evidenced from the voltammetric scans.

At 0.0V our findings show a copper-copper bond distance of 2.77 Å. As noted earlier, the coverage of copper at this potential is approximately one monolayer. The uncertainty in the coverage measurement has been already discussed. A copper-copper bond distance of 2.77 Å would make the copper adlayer commensurate with the platinum surface whose bond distance in the (111) direction is 2.75 Å. Thus the copper appears to form a (1x1) epitaxial adlayer on the substrate. From similar measurements for a full monolayer coverage of copper on gold(111) it was found that the copper-copper bond distance was identical to the gold-gold lattice spacing in

the (111) direction.[10b,j,k] Taking into account that we are employing σ-polarization an epitaxial arrangement of the copper adlayer on the platinum could place the copper in either bridge or three-fold-hollow sites. From our data we believe that the most likely position is in the three-fold-hollow sites. Out-of-plane experiments, currently underway, will allow an unambiguous determination of the adsorption site.

At an applied potential of 0.1V we again find oxygen in addition to copper as backscatterers. The copper-oxygen distance obtained was 2.17 Å which is essentially the same as that found at 0.0V. The position of the oxygens in relation to the copper adlayer and the platinum substrate is likely the same in both instances. The copper-copper near neighbor distance was found to be 2.85 Å. This value is larger than that of 2.77 Å obtained at 0.0V. At lower coverages the adlayer takes on a more open structure perhaps as a means of minimizing the coulombic repulsion arising from the fact that the ad-layer is not fully discharged. The expansion of the copper adlattice with respect to the platinum substrate (2.85 Å vs. 2.77 Å) would indicate that the platinum surface contributes less to the adlayer structure at lower coverages. However, it is difficult to reconcile how the surface would interact more strongly with the adlayer at higher coverage when such repulsion would be even stronger. If bisulfate anions are co-adsorbed (as suggested by Wieckowski) in the plane, they might cause a lattice expansion and in so doing stabilize the ad-layer. At full monolayer coverage, such an arrangement would be more difficult to accommodate. It should also be mentioned that a distance of 2.85 Å does not correspond to any structural parameter of platinum.

It is interesting to compare our results with those of White and Abruña.[10d] In that study, however, the platinum(111) surface was pretreated with iodine. Two interesting points to note from their study was that they found very pronounced copper-copper backscattering at only 0.3

monolayer and that the copper-copper bond distance was 2.88 Å. The similarity in the bond distances for both systems is striking. It suggests that the iodine overlayer played a significant role in ordering the copper adlayer at 0.3 monolayer and that clustering was present. In the present case, the ordering of the copper adlattice at 0.1V to give a copper-copper distance of 2.85 Å could be due to a similar effect, in this case elicited by the co-adsorption of bisulfate.

Another point of comparison is the work of Furtak *et al.*[10g] where they studied the structure of a copper monolayer on a platinum electrode. Their system differed from ours in a number of areas, the most significant being that they used, as an electrode, a platinum film evaporated onto optically flat glass. Since there is no mention of surface order, crystallographic orientation or mosaic spread it is hard to ascertain the long-range order (if any) of the surface. The surface is likely polycrystalline in nature and this might be the reason why they found a copper-copper distance of 2.59 Å. Because of its polycrystalline nature, it is likely that the substrate has very little influence in ordering the copper adlayer.

The structure at an applied potential of +0.2V is perhaps the most enigmatic. The coverage at +0.2V is approximately 0.5ML. As noted above, fitting the cluster of peaks in the radial distribution function, (figure 10a) required the use of three absorber-backscatterer pairs; Cu-O, Cu-Cu and Cu-Cu. The copper-oxygen bond distance of 1.99 Å is considerably smaller to the values obtained at the other two potentials studied.

Two copper-copper bond distances were found with values of 2.87 Å and 2.66 Å, respectively. The distance of 2.87 Å is virtually the same as that found at an applied potential of +0.1V. The other copper-copper bond length of 2.66 Å is considerably shorter than that obtained at +0.0V. There appear to be two distinct copper clusters on the surface. The previous work of White and Abruña[10d] on the submonolayer coverage of copper on an iodine pretreated

platinum(111) surface is arguably the most similar system to our XAS measurements at +0.2V. However, in their analysis only one copper-copper bond distance was found unlike the two Cu-Cu distances found in the present study.

However, the presence of two distinct copper clusters has been suggested by Kolb and co-workers[22, 23] Using optical techniques in the visible region, they measured the spectral dependence of the normalized reflectance change, $\Delta R/R$, for various copper coverage.[22, 23] Changes in $\Delta R/R$ are due to variations in the complex dielectric constant (ε", imaginary component) of the adsorbed species during the course of deposition. For copper deposition on Pt(111) and polycrystalline platinum they noted a sharp change in $\Delta R/R$ at a coverage of approximately 0.6ML. The absolute value for the adsorbates' absorption coefficient increases strongly and suddenly when the lateral interactions become more dominant. They have attributed the sharp change in $\Delta R/R$ to reconstruction of the copper adlayer. In addition, Arvia *et al.*[25a] and Furuya and Motoo[25b] found a competition between the electrodeposited overlayer of copper on platinum and the hydrogen electrode reactions. They postulated the existence of three-dimensional (3-D) clusters or islands on the surface at coverages slightly above a monolayer. Depending on the kinetics of the reconstruction process, our XAS measurements of two distinct copper-copper bond distances provides an atomically resolved window into this reconstruction mechanism.

The fits to the inverse filtered Fourier transform of the peaks reveal in all cases the presence of Cu-Cu scattering with the same coordination number of 6 within an accuracy of ± 20% and the formation of well ordered hexagonal structures. Since the effective coordination number of six remains virtually invariant with coverage, we conclude that there is a strong

tendency for clustering. The effective coordination number of nearest neighbor oxygens at 0.0V and at +0.1V is essentially the same and has a value of four. This is an unrealistically high value. However, considering the uncertainty (± 20%) a coordination number of three would place the oxygen in three-fold-hollow sites with respect to the copper ad-layer. The fact that scattering by oxygen is observed implies that there is a projection of the Cu-O bond in the plane; thus excluding atop sites. This would leave bridge and three-fold hollow sites as possible locations for the oxygen. However, the coordination number of two would only be consistent with bridge sites perhaps in an arrangement where the oxygen is being shared by adjacent copper atoms.

CONCLUSIONS

Surface EXAFS was used to study the potential dependent changes of the copper UPD layer on a clean and well-ordered Pt(111) surface. The charge derived from electrochemical measurements implied that at the three potential studied the electrodeposited copper was not completely discharged. The XANES analysis revealed similarities between the copper adlayer and the Cu_2O reference lending support to earlier findings of a partially discharged copper ad-layer. Oxygen is a persistent backscatterer and the Cu-O distance remained relatively unchanged at the at all potentials (0.0, +0.1 and +0.2V) studied. In the σ-polarization we observed intense copper-copper scattering at all potentials studied. At 0.0V we find the copper-copper distance to be 2.77 ± 0.03 Å with a coordination number of 6.3 ± 20%. At this potential the copper adlattice exhibits an epitaxial arrangement with the platinum(111) surface. At +0.1V the copper-copper bond distance is 2.85 ± 0.03 Å. Here the copper adlayer has expanded which is to be expected for a lower coverage. The coordination number is

approximately 6.2 ± 20%. At 0.0V and +0.1V we see the formation of well ordered hexagonal surface structures. The findings at +0.2V presents a window into the reconstruction of the adlayer with the presence of two copper-copper distances of 2.66 ± 0.03 Å and 2.87 ± 0.03 Å. Coordination numbers of 6.2 ± 20% at 2.66 and 5.7 ± 20% at 2.87 Å were found from the analysis. Two clusters with an hexagonal structure appear to be formed at approximately 0.5ML on a clean well-ordered Pt(111). The copper-copper distance was found to be strongly dependent on the coverage, whereas the copper-oxygen bond distance was not. Current studies are underway to determine the exact location of the copper and oxygen atom with respect to the substrate surface by probing both the Cu K edge and the Pt L edges.

ACKNOWLEDGEMENTS

Our work was generously supported by the National Science Foundation, the Office of Naval Research, and the Army Research Office. We thank Keith Bowers of the LAASP machine shop in aiding in the design and construction of the new Teflon electrochemical cell. Dr. Kenneth Finkelstein of the Cornell High Energy Synchrotron Source (CHESS) was especially helpful in the early stages of the experiments. The authors also acknowledge the assistance of D.L. Taylor, J. Hudson and S. Chen in collecting the data.

TABLE I.

EXAFS parameters. Bond lengths R, effective coordination number NN, Debye-Waller factor $\Delta\sigma$, and energy variation ΔE (accuracy: R, ± 0.03 Å; NN ± 20%). Electrochemical values. Applied potential E_{appl}, calculated charge Q (1ML = 420 $\mu C/cm^2$).

E_{pot} (Volt)	Q ($\mu C/cm^2$)	A-B	Radius (Å)	NN	$\Delta\sigma$ ($Å^2$)	ΔE (eV)
0.2	221.5	Cu-O	1.99	4.3	0.02	12.87
		Cu-Cu	2.66	6.2	0.0048	-3.26
		Cu-Cu	2.87	5.7	0.0051	-3.26
0.1	309.3	Cu-O	2.16	4.2	0.0084	15.00
		Cu-Cu	2.85	6.2	0.0123	2.26
0.0	345.9	Cu-O	2.14	4.1	0.0094	15.00
		Cu-Cu	2.77	6.3	0.0055	-0.82

REFERENCES:

1. (a) Zangwill, A. *Physics at Surfaces;* Cambridge University Press: Cambridge, U.K., 1988.

   (b) Adamson, A.W. *Physical Chemistry of Surfaces;* John Wiley: New York, 1982.

   (c) Somorjai, G.A. *Chemistry in Two Dimensions: Surfaces;* Cornell University Press: Ithaca, New York, 1981.

   (d) Hall, R.B.; Ellis, A.B., Eds., *Chemistry and Structure at Interfaces;* VCH Publishers Inc: Deerfield Beach, Fl, 1986.

2. (a) D.M. Kolb, *Advances in Electrochemistry and Electrochemical Engineering;* Gerischer, H., Tobias, C., Eds.; Pergamon: New York, 1978; Vol. 11, p125.

   (b) Adzic, R. *Advances in Electrochemistry and Electrochemical Engineering,* Gerischer, H., Tobias, C., Eds.; Pergamon: New York, 1985; Vol. 13, p159.

3. (a) Schultze, J.W.; Dickertmann, D. *Surf. Sci.* **1976,** *54,* 489.

   (b) Bewick, A.; Thomas, B. *J. Electroanal. Chem.* **1976,** *70,* 239.

4. (a) Beckmann, H.O.; Gerisher, H.; Kolb, D.M.; Lehnpfuhl, G. *Symp. Faraday Soc.,* **1977,** *12,* 51.

   (b) Stickney, J.L.; Rosasco, S.D.; Hubbard, A.T. *J. Electrochem. Soc.* **1984,** *131,* 260.

   (c) Hubbard, A.T. *Chem. Rev.* **1988,** *88,* 633 *and references therein.*

   (d) Leung, L.-W. H.; Gregg, T.W.; Goodman, D.W. *Langmuir* **1991,** *7,* 3205.

5. (a) Manne, S.; Hansma, P.K.; Massie, J.; Elings, V.B.; Gerwirth, A.A. *Science,* **1991,** *251,* 183.

   (b) Sashikata, K.; Furuya, N.; Itaya, K. *J. Electroanal. Chem.* **1991,** *316,* 361.

   (c) Hachiya, T.; Honbo, H.; Itaya, K. *J. Electroanal. Chem.* **1991,** *315,* 275.

   (d) Nichols, R.J.; Kolb, D.M.; Behm, R.J. *J. Electroanal. Chem.* **1991,** *313,* 109.

   (e) Nichols, R.J.; Beckmann, W.; Meyer, H.; Batina, N.; Kolb, D.M. *J. Electroanal. Chem.* **1992,** *330,* 381.

   (f) Chen, C.-H.; Vesecky, S.M.; Gewirth, A.A. *J. Am. Chem. Soc.* **1992,** *114,* 451.

6. Varga, K.; Zelenay, P.; Wieckowski, A. *J. Electroanal. Chem.* **1992**, *330*, 453.

7. (a) Krauskopf, E.K.; Rice, L.M.; Wieckowski, A. *J. Electroanal. Chem.* **1988**, *244*, 347.

(b) Wieckowski, A.; Zelenay, P.; Varga, K. *J. Chim. Phys.* **1991**, *88*, 1247.

8. Zelenay, P.; Wieckowski, A. *J. Electrochem. Soc.* **1992**, *139*, 2552.

9. H.D. Abruña, Ed. *Electrochemical Interfaces: Modern Techniques for In-Situ Interface Characterization;* VCH: New York, N.Y., 1991.

10. (a) Blum, L.; Abruña, H.D.; White, J.H.; Gordon II, J.G.; Borges, G.L.; Samant, M.G.; Melroy, O.R. *J. Chem. Phys.* **1986**, *85*, 6732.

(b) Melroy, O.R.; Samant, M.G.; Borges, G.L.; Gordon II, J.G.; Blum, L.; White, J.H.; Albarelli, M.J.; McMillan, M.; Abruña, H.D. *Lamgmuir* **1988**, *4*, 728.

(c) White, J.H.; Albarelli, M.J.; Abruña, H.D.; Blum, L.; Melroy, O.R.; Samant, M.G.; Borges, G.L.; Gordon II, J.G. *J. Phys. Chem.* **1988**, *92*, 4432.

(d) White, J.H.; Abruña, H.D. *J. Electroanal. Chem.* **1989**, *274*, 185.

(e) Abruña, H.D.; White, J.H.; Bommarito, G.M.; Albarelli, M.J.; Acevedo, D.; Bedzyk, M.J. *Rev. Sci. Instrum.* **1989**, *60*, 2529.

(f) Tourillon, G.; Guay, D.; Tadjeddine, A. *J. Electroanal. Chem.* **1990**, *289*, 263.

(g) Furtak, T.E.; Wang, L.; Creek, E.A.; Samamta, P.; Hayes, T.M.; Kendall, G.; Li, W.; Liang, G.; Lo, C.-M. *Electrochimca Acta* **1991**, *36*, 1869.

(h) McBreen, J.; O'Grady, W.E.; Tourillon, G.; Dartyge, E.; Fontaine, A. *J. Electroanal. Chem.* **1991**, *307*, 229.

(i) Durand, R.; Faure, R.; Aberdam, D.; Salem, C.; Tourillon, G.; Guay, D.; Ladoceur, M. *Electrochimca Acta* **1992**, *37*, 1977.

(j) Tadjeddine, A.; Guay, D.; Ladouceur, M.; Tourillon, G. *Phys. Rev. Lett.* **1991**, *66*, 2235.

(k) Tadjeddine, A.; Tourillon, G.; Guay, D. *Electrochimca Acta* **1991**, *36*, 1859.

11. (a) Toney, M.F.; Melroy, O.R. *Electrochemical Interfaces: Modern Techniques for In-Situ Interface Characterization*; Abruña, H.D., Ed.; VCH, Verlag Chemical: Berlin, 1991.

(b) Samant, M.G.; Toney, M.F.; Borges, G.L.; Blum, L.; Melroy, O.R. *J. Phys. Chem.*

1988, *92*, 220.

(c) Toney, M.F.; Gordon, J.G.; Samant, M.G.; Borges, G.L.; Wiesler, D.G.; Yee, D.; Sorensen, L.B. *Langmuir,* **1991**, *7*, 796.

12. (a) Bedzyk, M.J.; Bilderback, D.H.; Bommarito, G.M.; Caffrey, M.; Schildkraut, J.S. *Science,* **241,** 1788 (1988).

(b) Bedzyk, M.J.; Bommarito, G.M.; Caffrey, M.; Penner, T.L. *Science* **1990**, *248*, 52.

(c) Abruña, H.D.; Bommarito, G.M.; Acevedo, D. *Science* **1990**, *250*, 69.

(d) Bommarito, G.M.; Acevedo, D.; Rodriguez, J.R.; Abruña, H.D. *X-Rays in Material Analysis II: Novel Applications and Recent Developments*; Mills, D.M., Ed.; SPIE Proceedings; 1991; Vol. 1550, p156.

13. Kau, L.-S.; Spria-Solomon, D.J.; Penner-Hahn, J.E.; Hodgson, K.O.; Solomon, E.I. *J. Am. Chem. Soc.* **1987**, *109*, 6433.

14. Martens, G.; Rabe, P.; Schwentner, N.; Werner, A. *Phys. Rev. B* **1978**, *17*, 1481.

15. Lee, P.A.; Citrin, P.H.; Eisenberger, P.; Kincaid, B.M. *Rev. Mod. Phys.* **1981**, *53*, 769.

16. Clavilier, J. *J. Electroanal. Chem.* **1980**, *107*, 211.

17. Aberdam, D.; Durand, R.; Faure, R.; El-Omar, F. *Surf. Sci.* **1986**, *171*, 303.

18. Jaaf-Golze, K.A.; Kolb, D.M.; Scherson, D. *J. Electroanal. Chem.* **1986**, *200*, 353.

19. Kunimatsu, K.; Samant, M.G.; Seki, H. *J. Electroanal. Chem.* **1989**, *258*, 163.

20. Faguy, P.W.; Markovic, N.; Adzic, R.R.; Fierro, C.A.; Yeager, E.B. *J. Electroanal. Chem.* **1990**, *289*, 245.

21. Paffett, M.T.; Campbell, C.T.; Taylor, T.N.; Srinivasan, S. *Surf. Sci.* **1985**, *154*, 284.

22. Kolb, D.M.; Kötz, R. *Surf. Sci.* **1977**, *64*, 698.

23. Kolb, D.M.; Kötz, R.; Yamamoto, K. *Surf. Sci.* **1979**, *87*, 20.

24. (a) White, J.H.; Abruña, H.D. *J. Phys. Chem.* **1990**, *94*, 894.
(b) Michaelis, R.; Zei, M.S.; Zhai, R.S.; Kolb, D.M. *J. Electroanal. Chem.* **1992**, *299*, 339.

25. (a) Margheritis, D.; Salvarezza, R.C.; Giordano, M.C.; Arvia, A.J. *J. Electroanal. Chem.* **1987**, *229*, 327.

(b) Furuya, N.; Motoo, S. *J. Electroanal. Chem.* **1976**, *72*, 165.

26. Yee, H.S.; Abruña, H.D. *manuscript in preparation.*

FIGURE CAPTIONS:

Figure 1: Voltammogram of the Pt(111) electrode in the XAS cell. The electrolyte was 0.1M H_2SO_4. Scan rate, ν = 50 mV/sec. Reference electrode Ag/AgCl.

Figure 2: Voltammograms at Pt(111) electrodes in contact with a 50μM Cu^{2+} + 0.1M H_2SO_4 solution. Scan rate, ν = 2 mV/s. Reference electrode Ag/AgCl. (**a**) Measurements conducted under laboratory conditions. Dipping configuration. Only one face of Pt(111) exposed to the copper ion solution. (**b-d**) Voltammetric measurements made at the Cornell High Energy Synchrotron Source in the XAS cell. The entire crystal was exposed to the copper solution. (**b**) Potential was held at 0.0V during XAS measurement. (**c**) Potential was held at +0.1V during XAS measurement. (**d**) Potential was held at +0.2V during XAS measurement.

Figure 3: Cyclic voltammogram of copper underpotential deposition on Pt(111) in the presence of chloride: scan rate, ν = 2 mV/s; electrolyte, 0.1M H_2SO_4, 1mM of NaCl, and 50μM Cu^{2+}. Reference electrode Ag/AgCl.

Figure 4: A comparison of near-edge profile shapes around the Cu *K*-edge for reference compounds and measurements of Cu/Pt(111). (**a**) Cu/Pt(111) at 0.0V compared to the reference compounds. (**b**) Cu/Pt(111) at +0.1V. (**c**) Cu/Pt(111) at +0.2V.

Figure 5: EXAFS spectra of Cu/Pt(111) at the rest potential (+0.65V) of the system. Background measurement.

Figure 6: In-situ, x-ray absorption spectra around the copper *K*-edge for underpotentially deposited copper on a Pt(111) electrode in contact with a 50μM Cu^{2+}, 0.1M H_2SO_4 at various applied potentials. (**a**) Potential = 0.0V, Q = 346 μC/cm^2, Θ_{Cu} = 0.83. (**b**) Potential = +0.1V, Q = 309 μC/cm^2, Θ_{Cu} = 0.73. (**c**) Potential = +0.2V, Q = 222 μC/cm^2, Θ_{Cu} = 0.53.

Figure 7: Comparison of the in-situ, flourescence-detected absorption spectrum of copper underpotentially deposited on Pt(111) in the (**a**) absence and in the (**b**) presence of chloride. Electrolyte: 0.1M H_2SO_4, 1mM of NaCl, and 50μM Cu^{2+}.

Figure 8: (**a**) Radial distribution function (k^1 weighted) and (**b**) Raw EXAFS (filled circles) Fourier filtered and back-transformed (open circles) data and backscattering envelope (open triangles) at an applied potential of 0.0V.

Figure 9: (**a**) Radial distribution function (k^1 weighted) and (**b**) Raw EXAFS (filled circles) Fourier filtered and back-transformed (open circles) data and backscattering envelope (open triangles) at an applied potential of +0.1V.

Figure 10: (**a**) Radial distribution function (k^1 weighted) and (**b**) Raw EXAFS (filled circles) Fourier filtered and back-transformed (open circles) data and backscattering envelope (open triangles) at an applied potential of +0.2V.

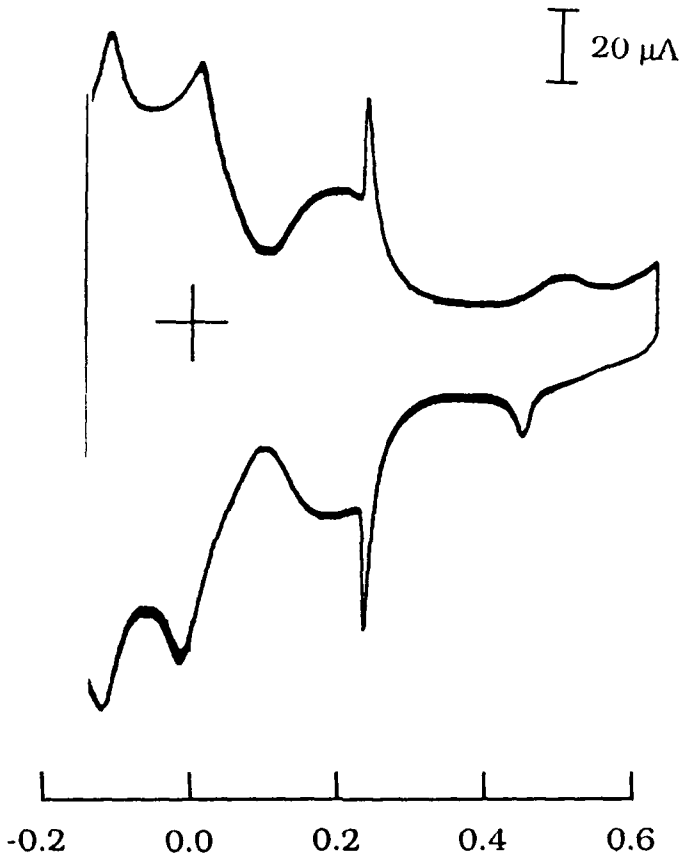

FIGURE 1

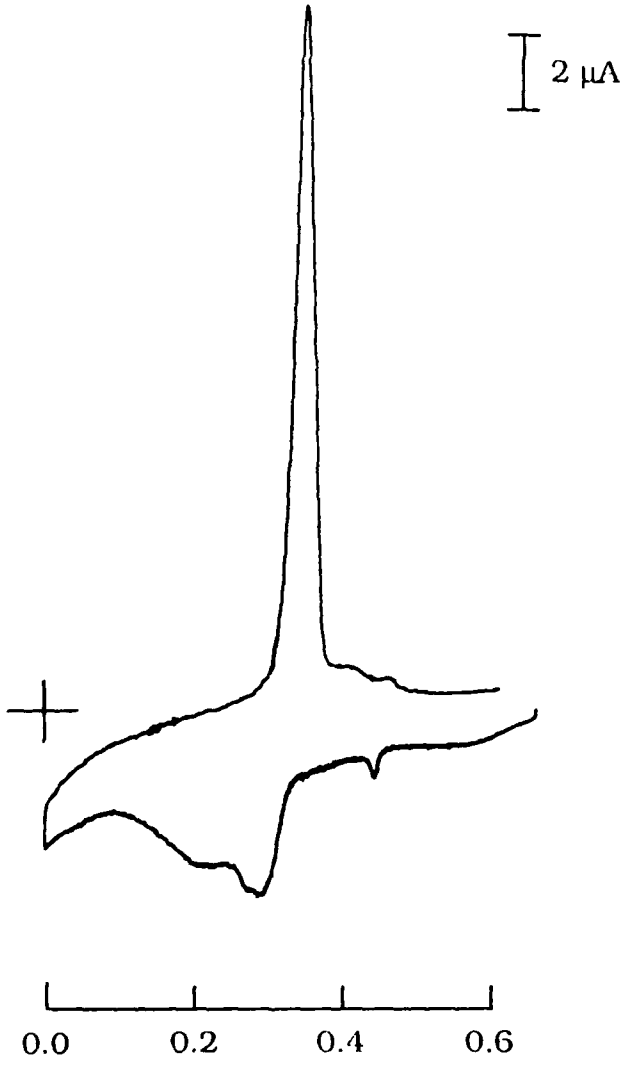

FIGURE 2a

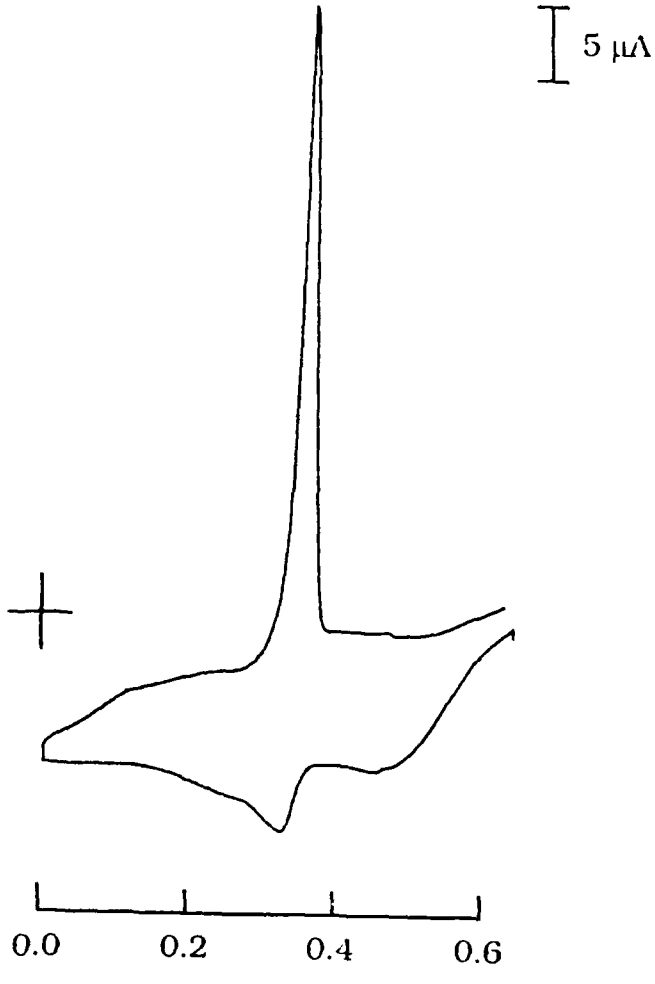

FIGURE 2b

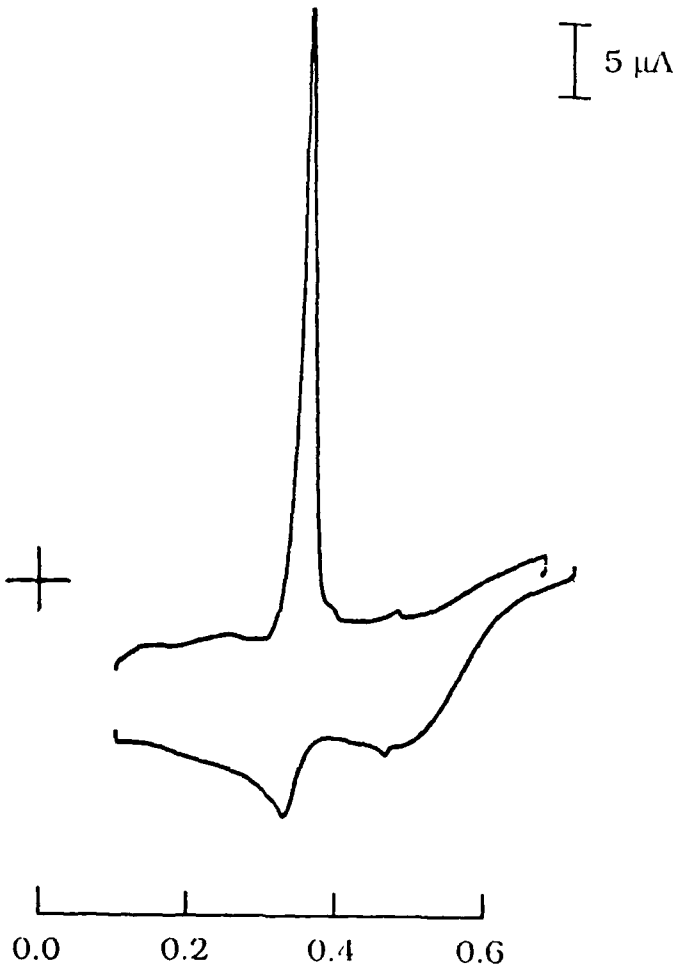

FIGURE 2c

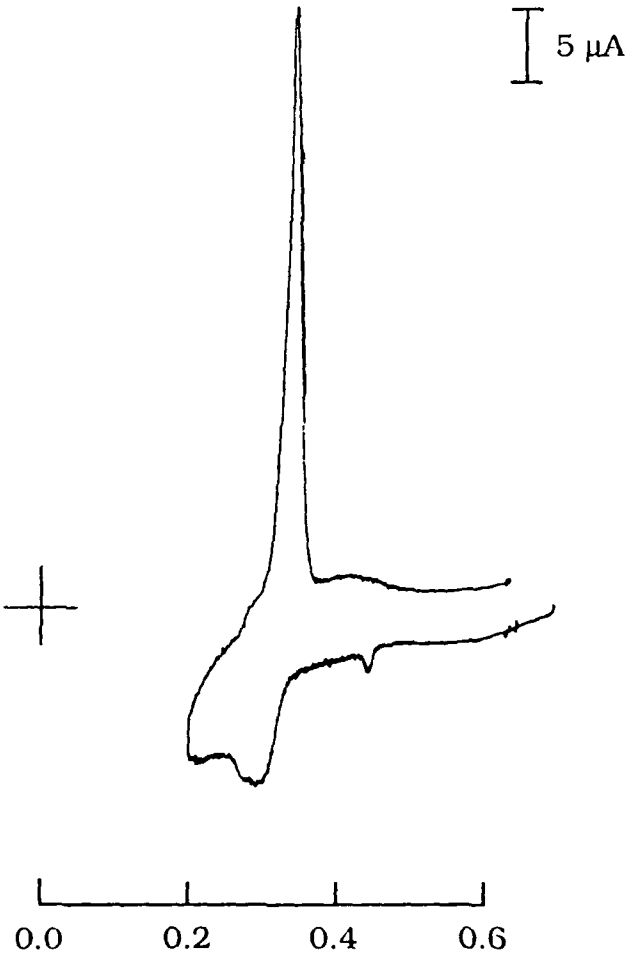

FIGURE 2d

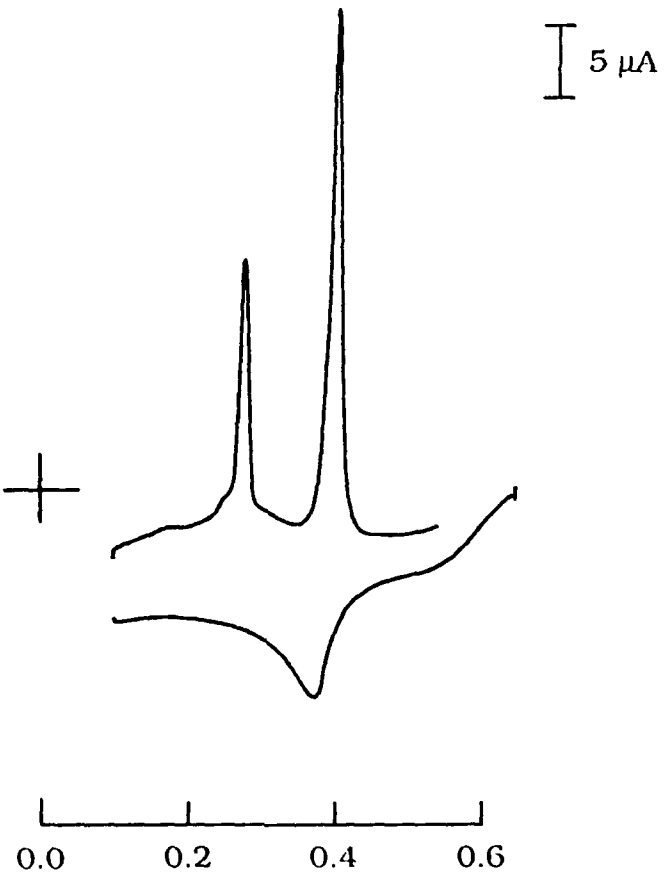

FIGURE 3

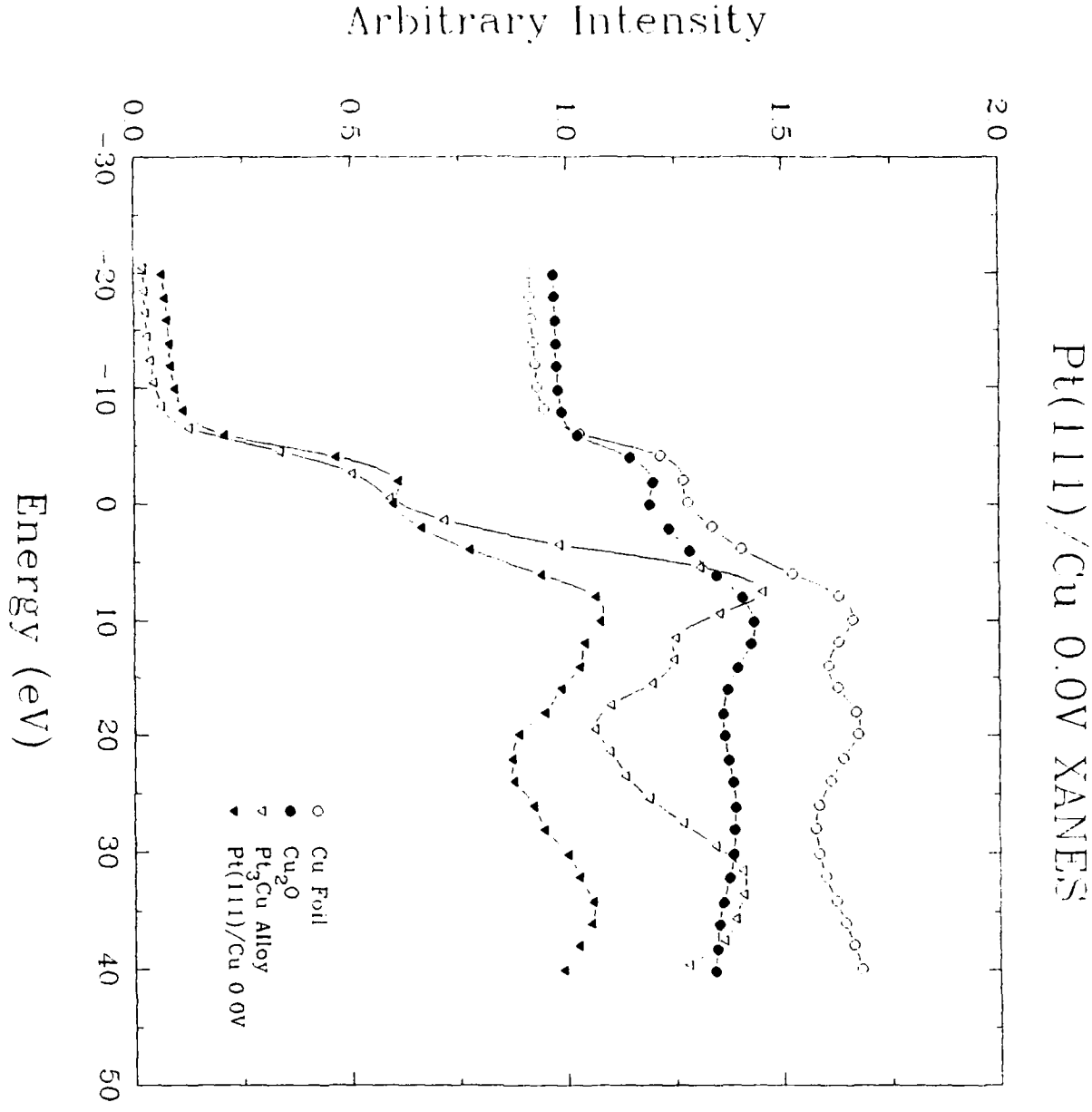
Pt(111)/Cu 0.0V XANES
Arbitrary Intensity
Energy (eV)
0.0
0.5
1.0
1.5
2.0
-30
-20
-10
0
10
20
30
40
50
Cu Foil
Cu_2O
Pt_3Cu Alloy
Pt(111)/Cu 0 0V

FIGURE 4a

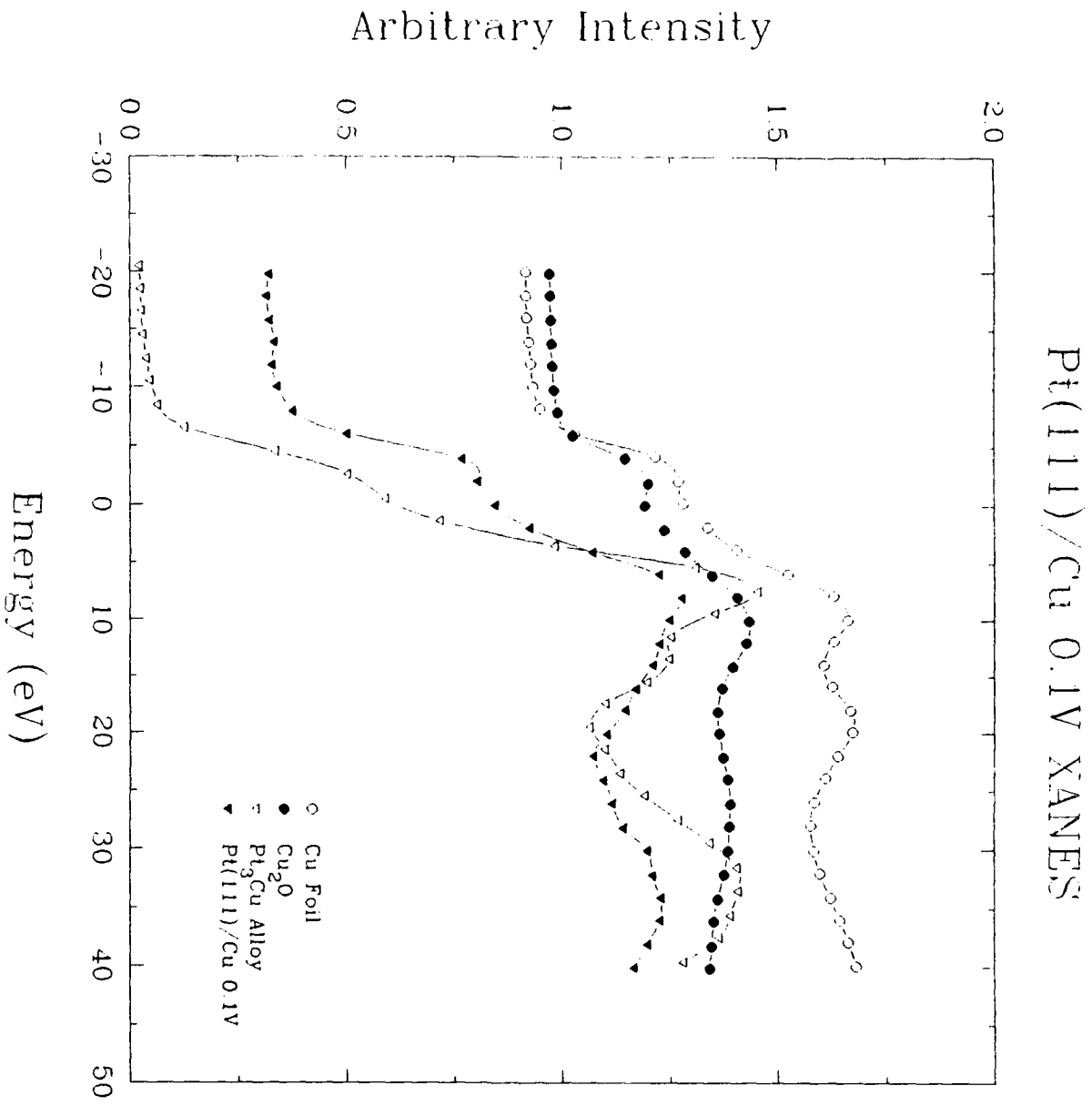
Arbitrary Intensity
0.0
0.5
1.0
1.5
2.0
-30
-20
-10
0
10
20
30
40
50
Energy (eV)
Pt(111)/Cu 0.1V XANES
Cu Foil
Cu2O
Pt3Cu Alloy
Pt(111)/Cu 0.1V

FIGURE 4b

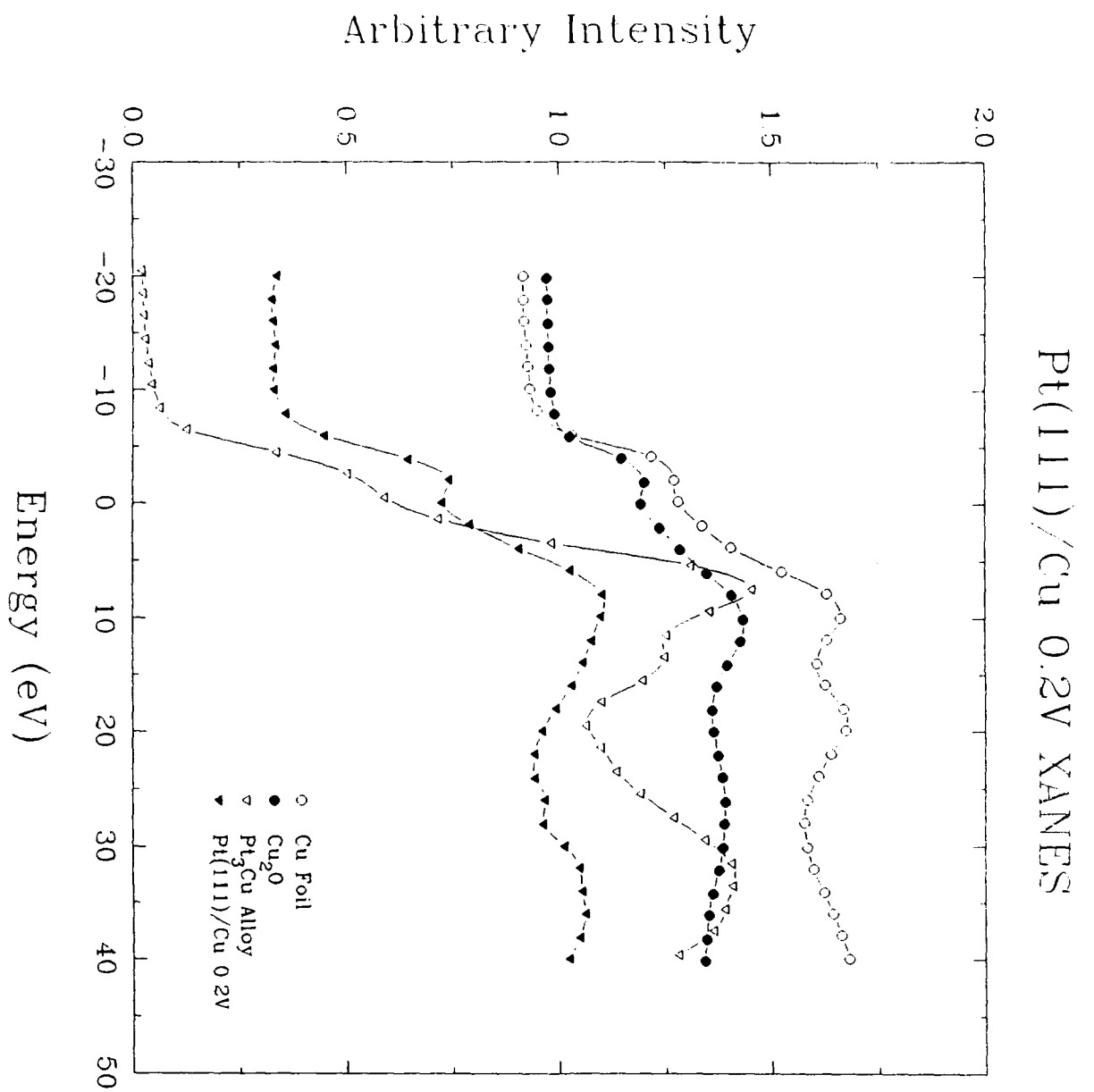
Arbitrary Intensity
0.0
0.5
1.0
1.5
2.0
-30
-20
-10
0
10
20
30
40
50
Energy (eV)
Pt(111)/Cu 0.2V XANES
Cu Foil
Cu_2O
Pt_3Cu Alloy
Pt(111)/Cu 0.2V

FIGURE 4c

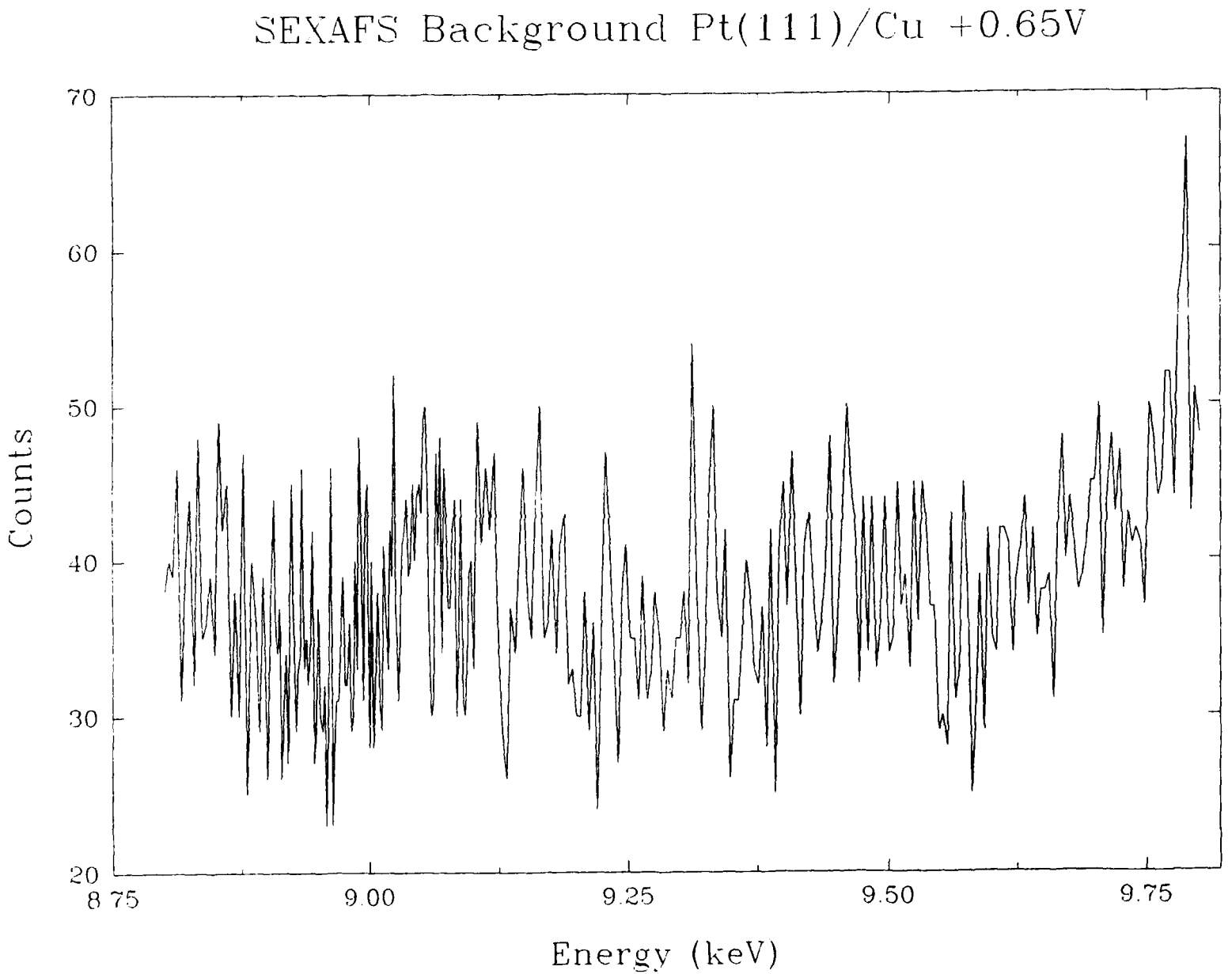
SEXAFS Background Pt(111)/Cu +0.65V
70
60
50
40
30
20
Counts
8.75
9.00
9.25
9.50
9.75
Energy (keV)

FIGURE 5

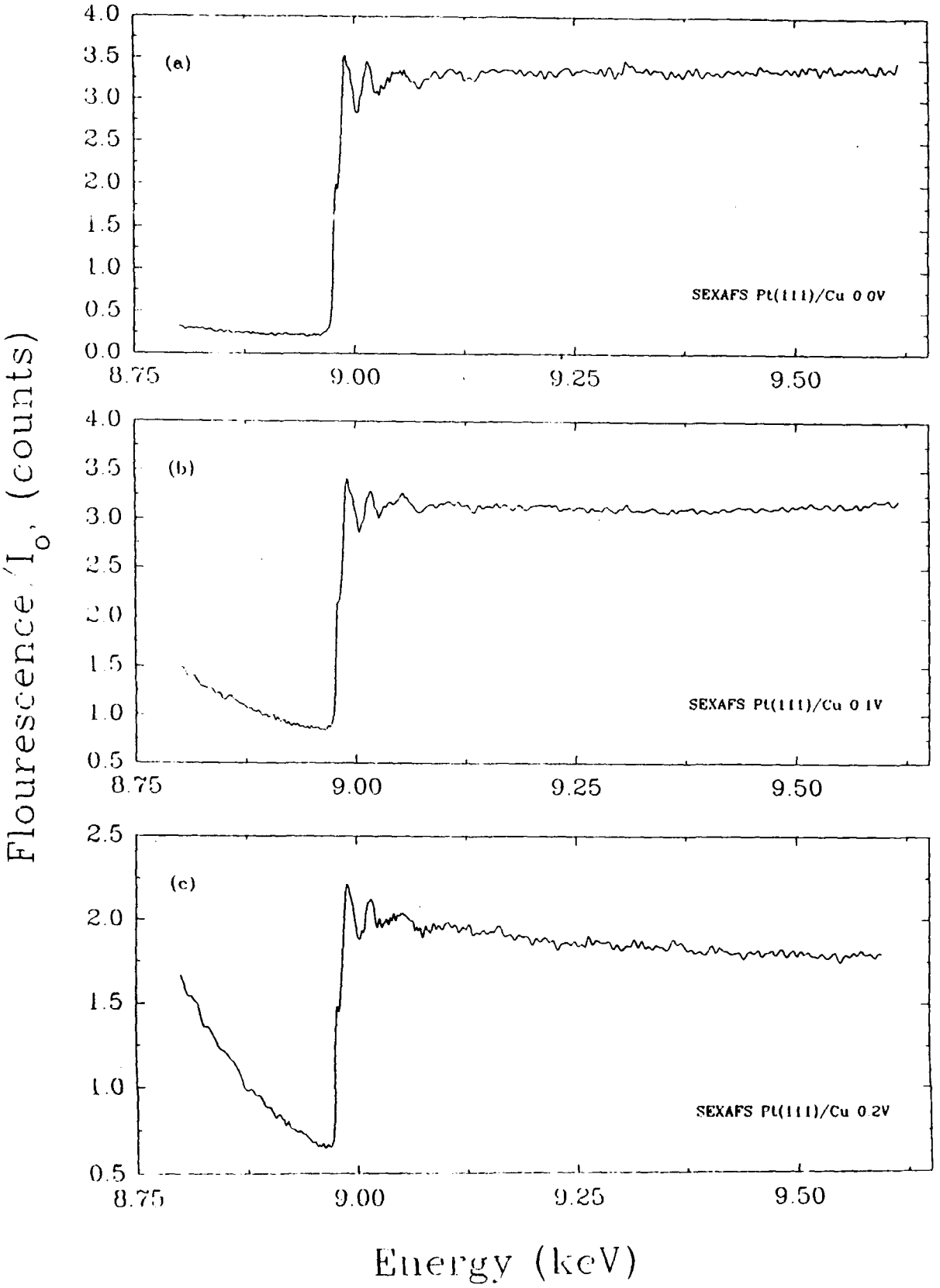
(a)
SEXAFS Pt(111)/Cu 0.0V
(b)
SEXAFS Pt(111)/Cu 0.1V
(c)
SEXAFS Pt(111)/Cu 0.2V
Flourescence I_o, (counts)
Energy (keV)
8.75
9.00
9.25
9.50

Figure 6

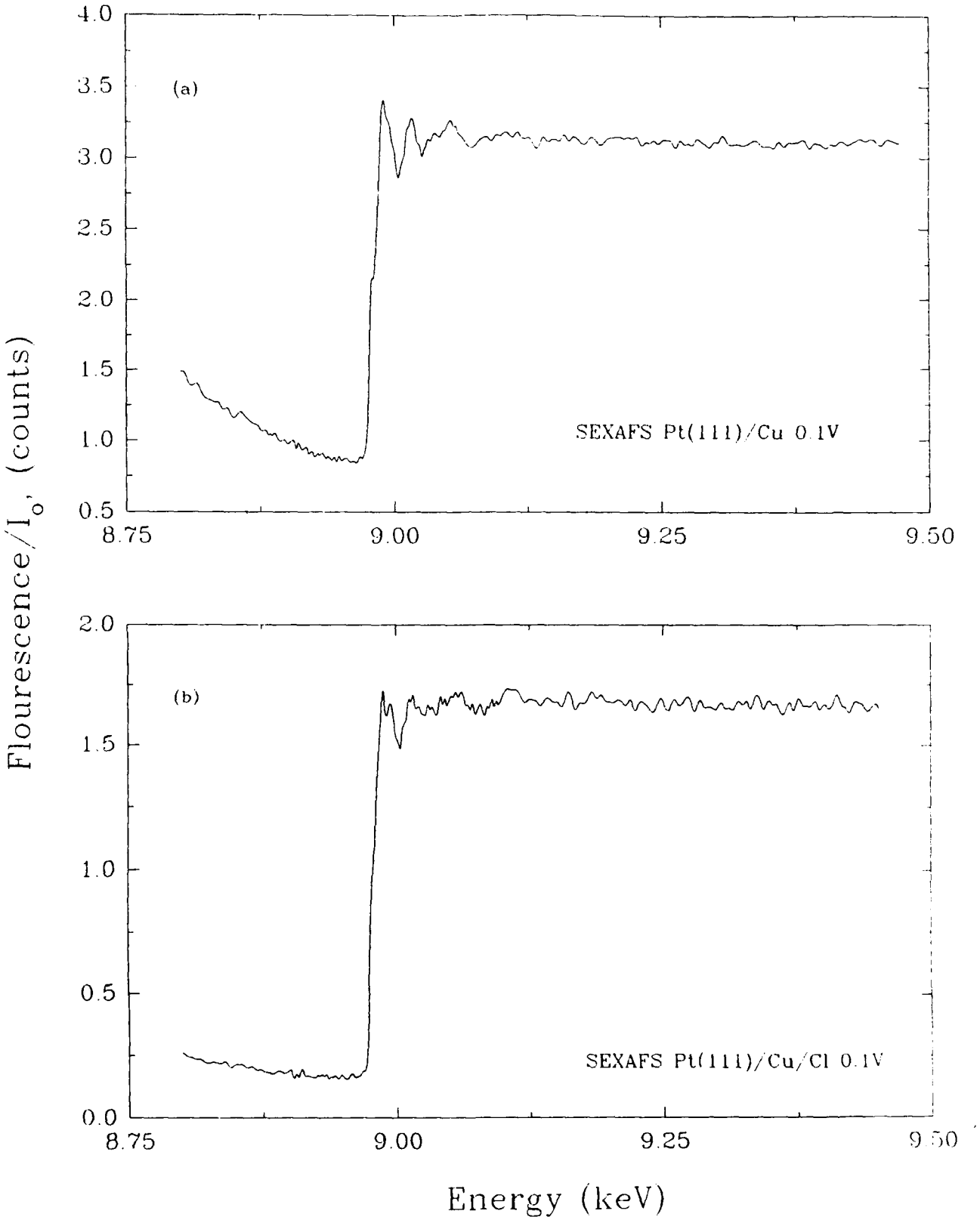
4.0
3.5
3.0
2.5
2.0
1.5
1.0
0.5
(a)
SEXAFS Pt(111)/Cu 0.1V
8.75
9.00
9.25
9.50
2.0
1.5
1.0
0.5
0.0
(b)
SEXAFS Pt(111)/Cu/Cl 0.1V
8.75
9.00
9.25
9.50
Flourescence/I_o, (counts)
Energy (keV)

FIGURE 7

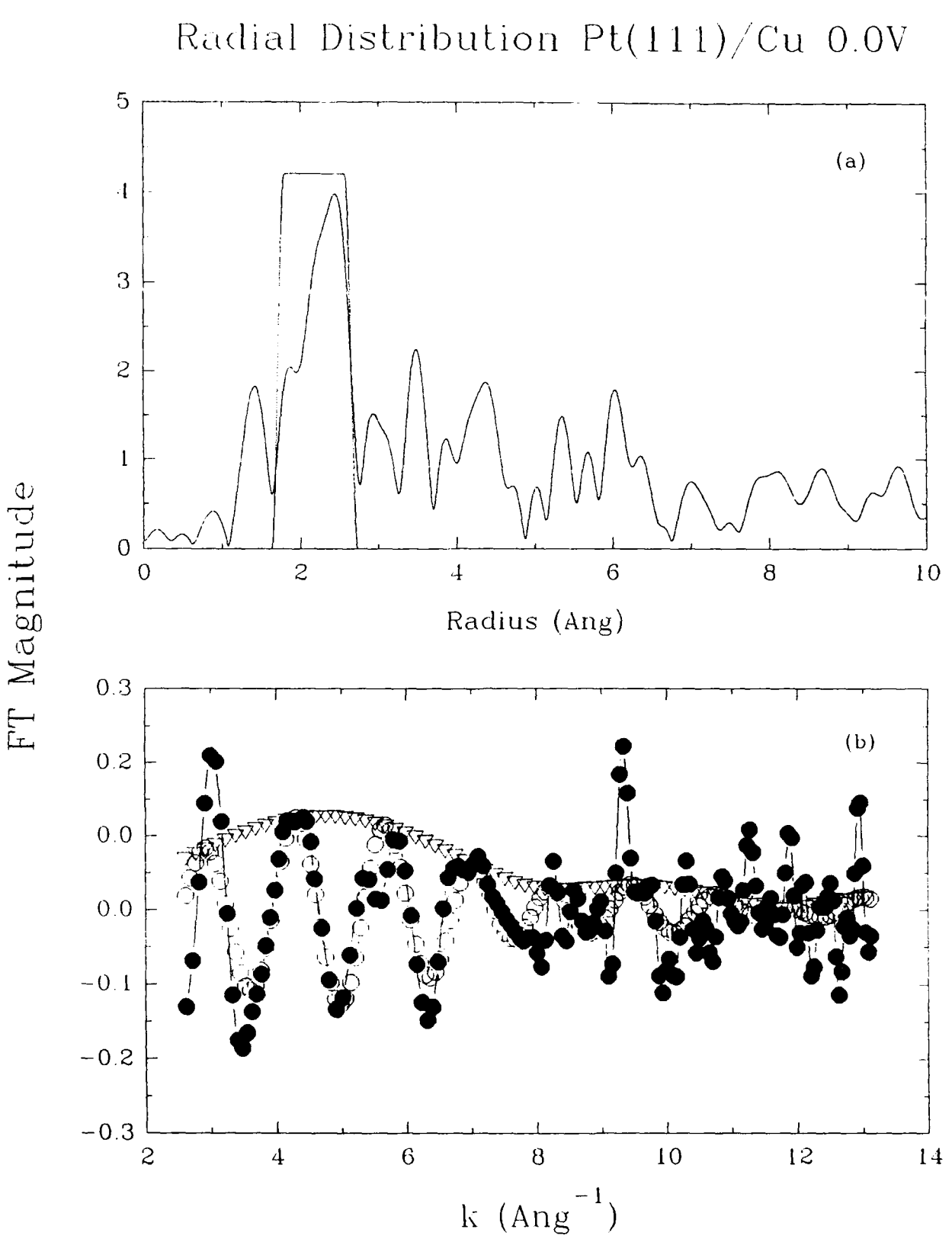
Radial Distribution Pt(111)/Cu 0.0V
(a)
FT Magnitude
Radius (Ang)
(b)
k (Ang^{-1})

FIGURE 8

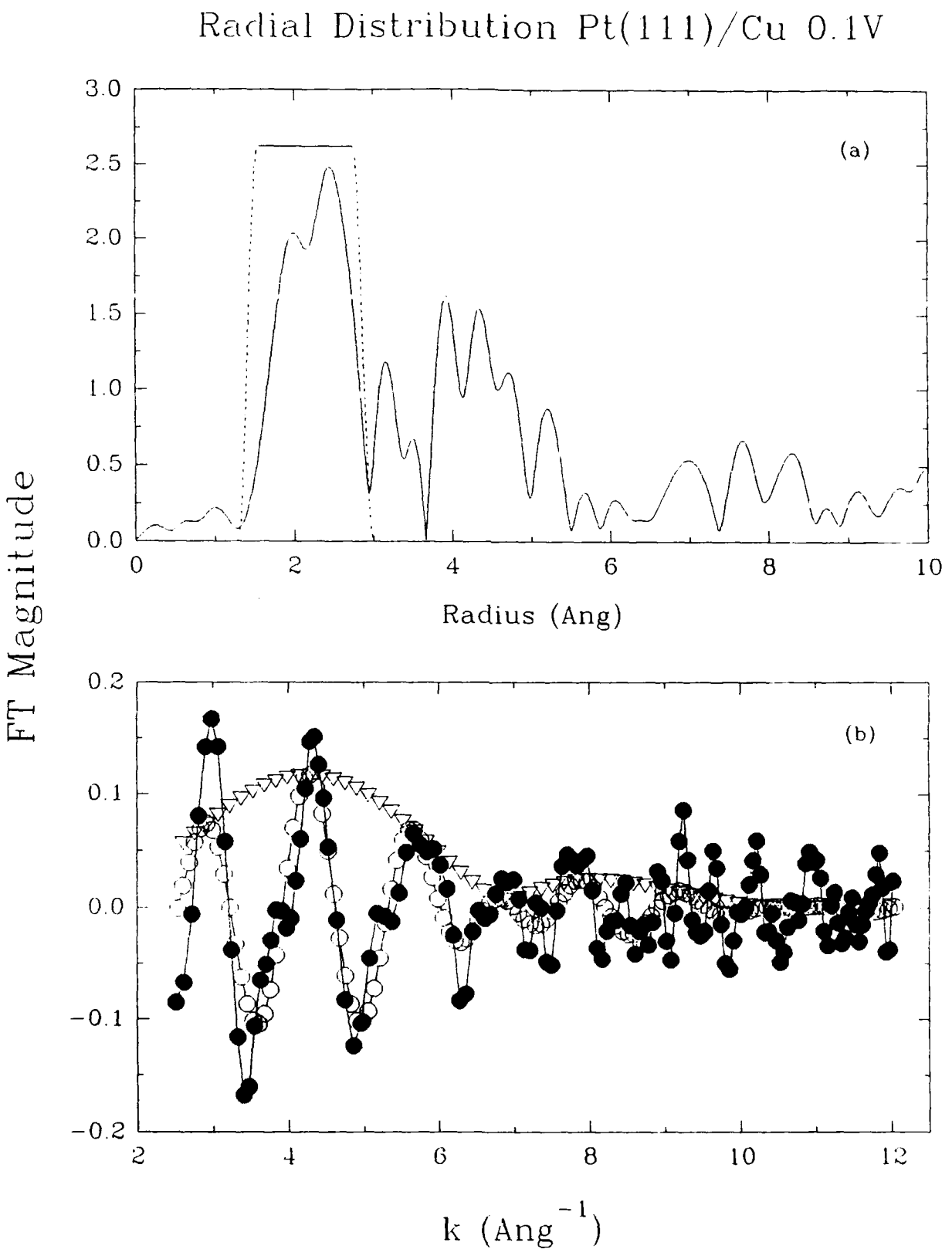
Radial Distribution Pt(111)/Cu 0.1V
FT Magnitude
3.0
2.5
2.0
1.5
1.0
0.5
0.0
(a)
0
2
4
6
8
10
Radius (Ang)
0.2
0.1
0.0
−0.1
−0.2
(b)
2
4
6
8
10
12
k (Ang^{-1})

FIGURE 9

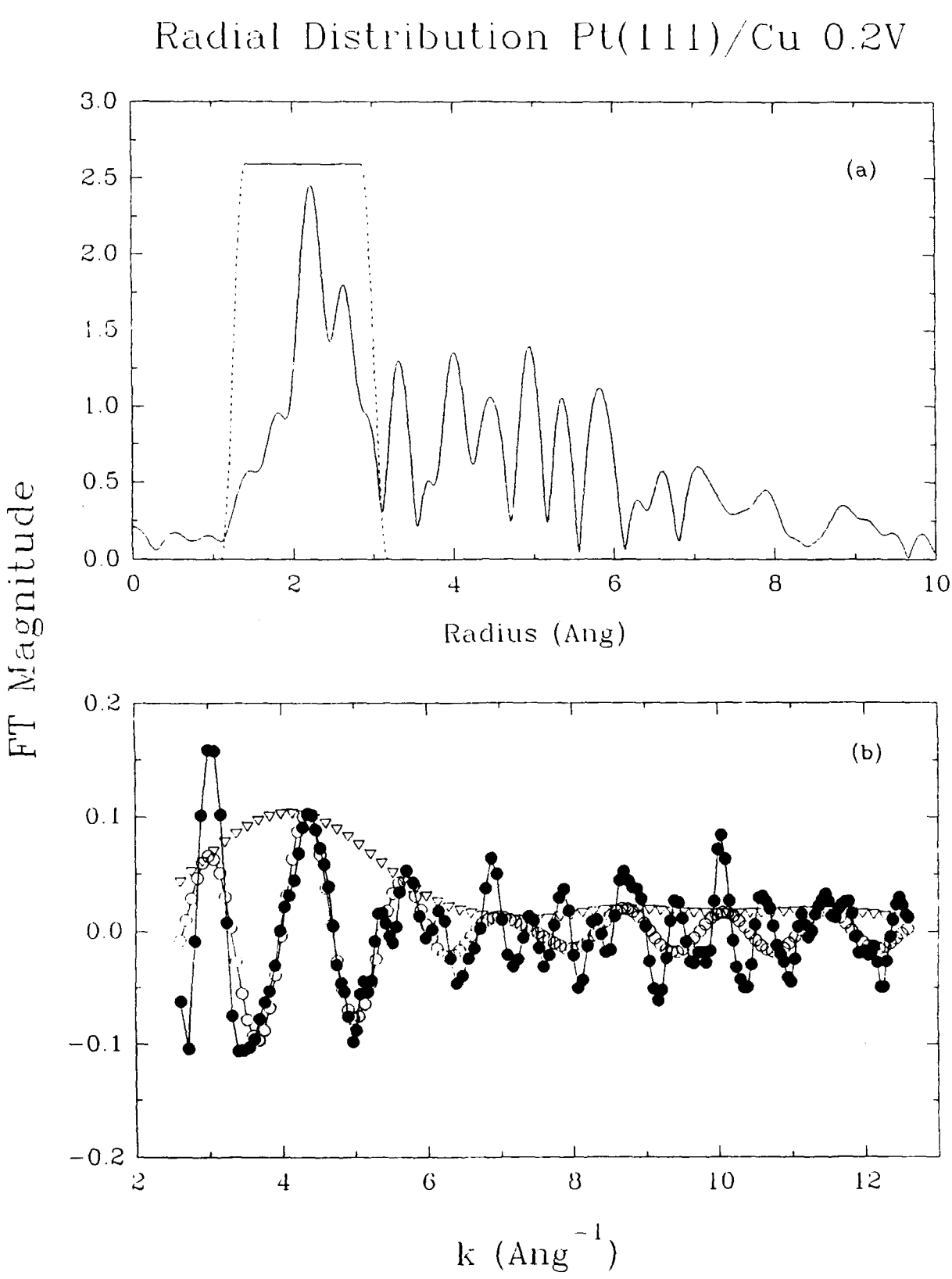
Radial Distribution Pt(111)/Cu 0.2V
FT Magnitude
3.0
2.5
2.0
1.5
1.0
0.5
0.0
0
2
4
6
8
10
Radius (Ang)
(a)
0.2
0.1
0.0
−0.1
−0.2
2
4
6
8
10
12
k (Ang^{-1})
(b)

FIGURE 10